

CHAPTER IV

RESULTS AND DISCUSSION

4.1 Formulation of MINLP Single Period Model

4.1.1 Model Components

A single period model was developed based on stage-wise superstructure proposed by Yee and Grossmann (1990). GAMS has been used to implement the model. Because the model is an MINLP involving linear binary variables, linear and non-linear continuous variables, so DICOPT was selected as a solver to solve the problem. This model subjected to minimize total annualized cost (TAC) where the trade-off of capital cost, area cost, and utility cost has been done simultaneously.

The components of a model in GAMS are shown as follows:

4.1.1.1 Sets

Sets are indices in algebraic representations that are used to identify the domain of a specific group of data. For example, i indicates hot stream i and j indicates cold stream j .

4.1.1.2 Data

Data is the input design parameters of the problem such as inlet/outlet temperatures, heat capacity flowrates, heat transfer coefficient, and economic parameter. There are several ways for data entry in GAMS such as declaring Parameter, Tables, or Scalars.

4.1.1.3 Variables

Variables are the decision variables which are optimized and determined by GAMS such as inter-stage temperatures, heat load, areas, and topology. It consists of binary variables and continuous variables.

4.1.1.4 Equations

Equations are the statements that express relationship between data and variables. The model has both equality constraint and non-equality constraint.

4.1.1.5 *Model and Solve Statement*

Model is the collection of equations declared by a chosen name and the solve statement will call for solver in order to solve the problem corresponding to objective of optimization (maximizing or minimizing).

4.1.1.6 *Other Components*

These GAMS's components are optional which are Display statements and Assignment of bound and/or initial values.

4.1.2 Assumptions

The MINLP type of model has more complexity and non-convex than the other types because of non-continuous and nonlinear functions in model. Hereby, some assumptions have to be made for simplicity.

4.1.2.1 *Isothermal-mixing*

In any stage, if the streams are splitted and pass through more than one exchanger, when they return to mix again before going to the next stage, they must have the same temperatures.

4.1.2.2 *Constant Heat Capacity Flowrates*

Heat capacity flowrate is a fluid property which is a function of temperature. Thus, in reality, the heat capacity flowrates in HEN would have been unconstant, but the constant heat capacity flowrates are assumed to reduce complexity of the model because the temperatures of the streams are changed and optimized throughout the model solving.

4.1.2.3 *No Stream Bypass*

Every splitted stream is needed to pass a heat exchanger. The important reason is that it cannot be splitted and mixed without passing any heat exchanger because of the assumption of isothermal-mixing.

4.1.2.4 *No Split Stream Passing Through more than One Heat Exchanger*

The splitted streams are allowed to pass through only one exchanger. A series of heat exchangers for a splitted stream is not included.

4.1.2.5 Utilities are Places at the End of Each Stream

The utility exchangers are placed at the end of each stream only. The inter-stage utility is not included.

4.1.3 Formulations

The MINLP single period model consists of a series of equations as expressed below from Eq. 4.1-4.26. For more detailed description of each equation, see section 2.2.3.2.

4.1.3.1 Overall Energy Balance of Each Stream

$$[Th_{in}(i) - Th_{out}(i)].FCph(i) = \sum_{k \in ST} \sum_{j \in CP} q(i, j, k) + q_{cu}(i) \quad i \in HP \quad (4.1)$$

$$[Tc_{in}(j) - Tc_{out}(j)].FCpc(j) = \sum_{k \in ST} \sum_{i \in HP} q(i, j, k) + q_{hu}(j) \quad j \in CP \quad (4.2)$$

4.1.3.2 Energy Balance at Each Stage

$$[th(i, k) - th(i, k + 1)].FCph(i) = \sum_{j \in CP} q(i, j, k) \quad k \in ST, i \in HP \quad (4.3)$$

$$[tc(j, k) - tc(j, k + 1)].FCpc(j) = \sum_{i \in HP} q(i, j, k) \quad k \in ST, j \in CP \quad (4.4)$$

4.1.3.3 Assignment of Inlet Temperatures

$$Th_{in}(i) = th(i, 1) \quad i \in HP \quad (4.5)$$

$$Tc_{in}(j) = tc(j, NOK + 1) \quad j \in CP \quad (4.6)$$

4.1.3.4 Monotonic Decrease in Temperatures

$$th(i, k) \geq th(i, k + 1) \quad k \in ST, i \in HP \quad (4.7)$$

$$tc(j, k) \geq tc(j, k + 1) \quad k \in ST, j \in CP \quad (4.8)$$

$$th(i, NOK + 1) \geq Th_{out}(i) \quad i \in HP \quad (4.9)$$

$$TC_{out}(j) \geq tc(j, 1) \quad j \in CP \quad (4.10)$$

4.1.3.5 Hot and Cold Utility Loads

$$[th(i, NOK + 1) - Th_{out}(i)]. FCph(i) = qcu(i) \quad i \in HP \quad (4.11)$$

$$[TC_{out}(j) - tc(j, 1)]. FCpc(j) = qhu(j) \quad j \in CP \quad (4.12)$$

4.1.3.6 Logical Constraints

$$q(i, j, k) - Q_{up} \cdot z(i, j, k) \leq 0 \quad i \in HP, j \in CP, k \in ST \quad (4.13)$$

$$qcu(i) - Q_{up} \cdot zcu(i) \leq 0 \quad i \in HP \quad (4.14)$$

$$qhu(j) - Q_{up} \cdot zhu(j) \leq 0 \quad j \in CP \quad (4.15)$$

where $z(i, j, k), zcu(i), zhu(i) \in \{0, 1\}$

4.1.3.7 Minimum Approach Temperature Constraints

$$dt(i, j, k) \leq th(i, k) - tc(j, k) + DT_{up} \cdot (1 - z(i, j, k))$$

$$i \in HP, j \in CP, k \in ST \quad (4.16)$$

$$dt(i, j, k + 1) \leq th(i, k + 1) - tc(j, k + 1) + DT_{up} \cdot (1 - z(i, j, k))$$

$$i \in HP, j \in CP, k \in ST \quad (4.17)$$

$$dtku(i) \leq th(i, NOK + 1) - Tcu_{out} + DT_{up} \cdot (1 - zcu(i)) \quad i \in HP \quad (4.18)$$

$$dthu(j, p) \leq Thu_{out} - tc(j, 1, p) + DT_{up} \cdot (1 - zhu(i)) \quad j \in CP \quad (4.19)$$

4.1.3.8 Log Mean Temperature Difference

$$LMTD(i, j, k) = \left[dt(i, j, k) \cdot dt(i, j, k + 1) \cdot \frac{dt(i, j, k) + dt(i, j, k + 1)}{2} \right]^{1/3}$$

$$i \in HP, j \in CP, k \in ST \quad (4.20)$$

$$LMTDHU(j) = \left[dthur(j) \cdot dthul(j) \cdot \frac{dthur(j) + dthul(j)}{2} \right]^{1/3} \quad j \in CP \quad (4.21)$$

$$LMTDCU(i) = \left[dtcur(i) \cdot dtcul(i) \cdot \frac{dtcur(i) + dtcul(i)}{2} \right]^{1/3} \quad i \in HP \quad (4.22)$$

4.1.3.9 Heat Exchanger Area Calculations

$$Area(i, j, k) \geq \frac{q(i, j, k)}{LMTD(i, j, k).U(i, j)} \quad i \in HP, j \in CP, k \in ST \quad (4.23)$$

$$AreaHU(j) \geq \frac{qhu(j)}{LMTDHU(j).UHU(j)} \quad j \in CP \quad (4.24)$$

$$AreaCU(i) \geq \frac{qcu(i)}{LMTDCU(i).UCU(i)} \quad i \in HP \quad (4.25)$$

4.1.3.10 Objective Function

$$\begin{aligned} \min TAC = AF & \left[\sum_{i \in HP} \sum_{j \in CP} \sum_{k \in ST} C_f.z(i, j, k) + \sum_{i \in HP} \sum_{CU} C_f.zcu(i) \right. \\ & \left. + \sum_{j \in CP} \sum_{HU} C_f.zhu(j) \right] + AF. \sum_{i \in HP} \sum_{j \in CP} \sum_{k \in ST} C.Area(i, j, k)^B \\ & + AF. \sum_{j \in CP} C.AreaHU(j)^B + AF. \sum_{i \in HP} C.AreaCU(i)^B \\ & + \sum_{i \in HP} C_{cu}qcu(i) + \sum_{j \in CP} C_{hu}qhu(j) \end{aligned} \quad (4.26)$$

The set of all formulations shown above would be used as original model for extension to other models in both sequential and simultaneous approaches. It was approved by a simple simulated case study which illustrated that the model could run properly.

4.2 Sequential Approach for Multiperiod HEN Synthesis

4.2.1 Algorithm

Multiperiod HEN synthesis usually results from the assembly of HEN from each period. The concept of this proposed sequential method is that HEN will be generated for each period separately by using either original MINLP single period model or modified model from section 4.1. Figure 4.1 shows the proposed sequential approach algorithm.

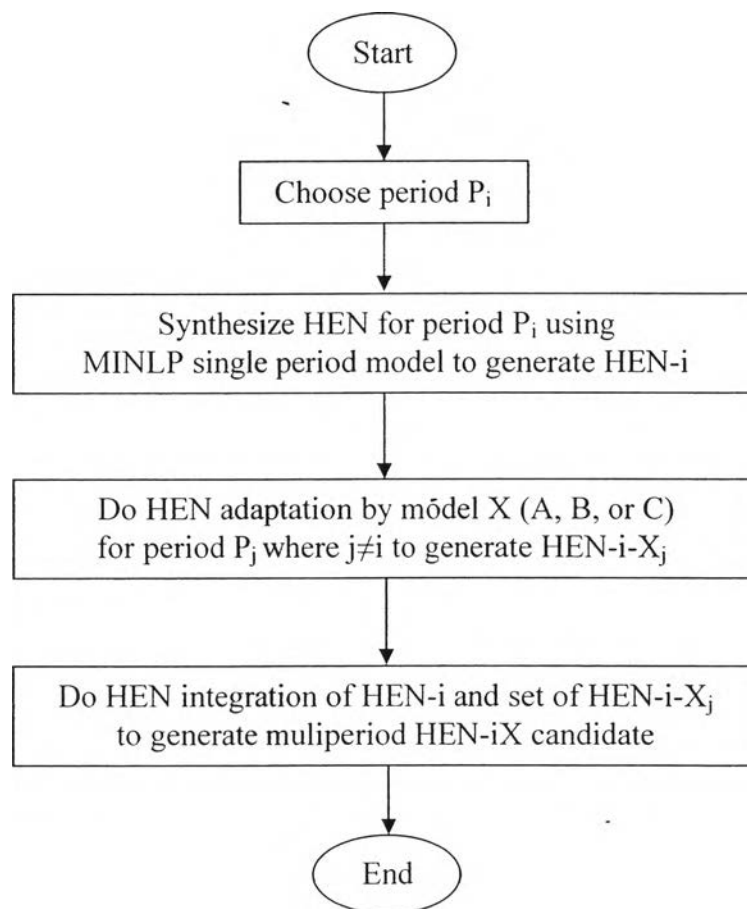


Figure 4.1 Algorithm of sequential approach for multiperiod HEN synthesis.

4.2.1.1 Single Period HEN Synthesis

In this step, the MINLP single period model from section 4.1 is used to generate an initial HEN for period P_i . Note that, for multiperiod problem, there are stream properties for more than one period, but only one of those periods will be chosen to be the input data for this step. For example, as illustrate in Figure 4.1, period P_i is used as the starting point. For simplification, this generated HEN is so-called HEN-i which means HEN for period P_i .

4.2.1.2 HEN Adaptation

This procedure is to adapt and apply the existing initial HEN from the previous step by maintaining the structure as much as possible. As a result, the adapted HEN will be able to operate for the particular periods. Hence, the input stream data for this step is the data of remaining periods (P_j) besides period P_i . There are three different modified models can be used in HEN adaptation which are model A, B, and C. As mentioned before, each model was modified from original MINLP single period model from section 4.1. They have different algorithms, but mainly retain the structure of the initial HEN. The principles of those three modified models are described as follows:

A. Model A

Model A is the MINLP single period model with fixed process exchanger area. The principle of this model is to keep the same topology and area of process-process exchangers only. The location of existing utility exchanger is also similar to initial HEN. But while solving, model A will allow new utility exchanger to be added and some of utility exchangers may need to switch between hot and cold utility when changing the operational periods. The objective function of this model is to minimize total additional area of utility exchangers as shown in Eq. 4.27.

$$\begin{aligned}
\text{Total additional area} = & \sum_{j \in CP} \max [0, \text{Area}_{HU_new}(j) - \text{Area}_{HU_old}(j)] \\
& + \sum_{i \in HP} \max [0, \text{Area}_{CU_new}(i) - \text{Area}_{CU_old}(i)]
\end{aligned} \tag{4.27}$$

B. Model B

Model B is the NLP single period model with fixed exchanger topology. The concept of this model is to maintain the old structure of initial HEN and not to allow the addition or removal of any heat exchangers. However, some heat exchangers may have to change their areas to satisfy heat balance. The objective function of this model is least square of area change as shown in Eq. 4.28.

$$\begin{aligned}
\text{Total area change} = & \sum_{i \in HP} \sum_{j \in CP} \sum_{k \in ST} [\text{Area}_{new}(i, j, k) - \text{Area}_{old}(i, j, k)]^2 \\
& + \sum_{j \in CP} [\text{Area}_{HU_new}(j) - \text{Area}_{HU_old}(j)]^2 \\
& + \sum_{i \in HP} [\text{Area}_{CU_new}(i) - \text{Area}_{CU_old}(i)]^2
\end{aligned} \tag{4.28}$$

C. Model C

Model C is the NLP single period model with fixed exchanger topology. This model is indeed similar to model B except the objective function. The objective function of this model is to minimize additional area and does not take into account the change of reduced area. The equation is illustrated in Eq. 4.29.

Total additional area

$$\begin{aligned}
&= \sum_{i \in HP} \sum_{j \in CP} \sum_{k \in ST} \max [0, Area_{new}(j, j, k) - Area_{old}(i, j, k)] \\
&\quad + \sum_{j \in CP} \max [0, Area_{HU_new}(j) - Area_{HU_old}(j)] \\
&\quad + \sum_{i \in HP} \max [0, Area_{CU_new}(i) - Area_{CU_old}(i)]
\end{aligned} \tag{4.29}$$

Note that in these three modified models, the other variables such as temperatures and heat loads are not fixed. Thus, they may have to change due to the variation of each period condition. And because these variables do not directly affect the cost of HEN, they are not included in the objective function.

From Figure 4.1, after HEN-i is adapted in the second step, it is named as HEN-i-X_j, where X refers to the modified model which can be either A, B, or C and j means that HEN is designed for period P_j.

4.2.1.3 HEN Integration

From HEN synthesis and HEN adaptation steps, HENs for each particular period are generated. Definitely the plant would not like to build all of those HENs for each period. Therefore, they have to be integrated to obtain a HEN which can operate for every condition. This is so-called multiperiod HEN-iX where i indicates the chosen period P_j in HEN synthesis step and X represents the modified model being used in HEN adaptation step. The integration can be done by using these two concepts:

A. Every match that exists at least one time in any period has to exist in multiperiod HEN. In other words, every heat exchanger that is needed in each period will be included in multiperiod HEN even though it is used for only one or less than N period.

B. Considering the area of each exchanger in multiperiod HEN, the maximum required area among all period will be selected. Because if the maximum area is not used, the area may not enough for heat to transfer in the period which requires more heat load.

When multiperiod HEN is obtained from HEN integration step, the actual TAC has to recalculate by using Eq. 4.30:

$$\begin{aligned}
 TAC = AF & \left[\sum_{i \in H P} \sum_{j \in C P} \sum_{k \in S T} C_f \cdot z(i, j, k) + \sum_{i \in H P} \sum_{C U} C_f \cdot z_{c u}(i) + \sum_{j \in C P} \sum_{H U} C_f \cdot z_{h u}(j) \right] \\
 & + AF \cdot \sum_{i \in H P} \sum_{j \in C P} \sum_{k \in S T} C \cdot \text{Area}_{\max}(i, j, k)^B + AF \cdot \sum_{j \in C P} C \cdot \text{Area}_{H U}_{\max}(j)^B \\
 & + AF \cdot \sum_{i \in H P} C \cdot \text{Area}_{C U}_{\max}(i)^B + \sum_{p \in P R} \frac{DOP(p)}{TOP} \sum_{j \in C P} C_{h u} q_{h u}(j, p) \\
 & + \sum_{p \in P R} \frac{DOP(p)}{TOP} \sum_{i \in H P} C_{c u} q_{c u}(i, p)
 \end{aligned} \tag{4.30}$$

4.2.2 Case Study

The case study was adapted from Verheyen and Zhang (2006). It is the vacuum gas oil (VGO) hydrotreating unit in oil refinery. This unit can simultaneously treat some impurities such as sulfur and convert some fraction of VGO to more valuable products. Hydrotreating is a catalytic reaction. The catalyst used in the process will gradually deactivate until a certain time before regeneration. During the deactivation, rate of reaction will decrease. Therefore, to compensate the deactivation of catalyst, the increase of temperature will help keep the reaction at approximately the same rate. In this case study there are three periods which are start-of-run (SOR), mid-of-run (MOR), and end-of-run (EOR). The change of temperature in each period will cause the variation of outlet compositions and flowrates.

Table 4.1, 4.2, and 4.3 shows stream properties for period SOR, MOR, and EOR respectively. Since the data of heat transfer coefficient was not provided, it will be assumed. Furthermore, the duration of each period is assumed to be equal.

Table 4.1 Stream properties for SOR

| Stream | Inlet temperature (°C) | Outlet temperature (°C) | Heat capacity flowrate (kW/K) | Heat transfer coefficient (kW/m ² .°C) |
|--------|------------------------|-------------------------|-------------------------------|---|
| H1 | 393 | 60 | 201.6 | 2.0 |
| H2 | 160 | 40 | 185.1 | 2.0 |
| H3 | 354 | 60 | 137.4 | 2.0 |
| C1 | 72 | 356 | 209.4 | 1.5 |
| C2 | 62 | 210 | 141.6 | 1.5 |
| C3 | 220 | 370 | 176.4 | 2.0 |
| C4 | 253 | 284 | 294.4 | 2.0 |
| HU | 400 | 399 | - | 2.0 |
| CU | 15 | 20 | - | 1.0 |

Table 4.2 Stream properties for MOR

| Stream | Inlet temperature (°C) | Outlet temperature (°C) | Heat capacity flowrate (kW/K) | Heat transfer coefficient (kW/m ² .°C) |
|--------|------------------------|-------------------------|-------------------------------|---|
| H1 | 406 | 60 | 205.0 | 2.0 |
| H2 | 160 | 40 | 198.8 | 2.0 |
| H3 | 362 | 60 | 136.4 | 2.0 |
| C1 | 72 | 365 | 210.3 | 1.5 |
| C2 | 62 | 210 | 141.0 | 1.5 |
| C3 | 220 | 370 | 175.4 | 2.0 |
| C4 | 250 | 290 | 318.7 | 2.0 |
| HU | 400 | 399 | - | 2.0 |
| CU | 15 | 20 | - | 1.0 |

Table 4.3 Stream properties for EOR

| Stream | Inlet temperature (°C) | Outlet temperature (°C) | Heat capacity flowrate (kW/K) | Heat transfer coefficient (kW/m ² .°C) |
|--------|------------------------|-------------------------|-------------------------------|---|
| H1 | 420 | 60 | 208.5 | 2.0 |
| H2 | 160 | 40 | 175.2 | 2.0 |
| H3 | 360 | 60 | 134.1 | 2.0 |
| C1 | 72 | 373 | 211.1 | 1.5 |
| C2 | 62 | 210 | 140.5 | 1.5 |
| C3 | 220 | 370 | 174.5 | 2.0 |
| C4 | 249 | 286 | 271.2 | 2.0 |
| HU | 400 | 399 | - | 2.0 |
| CU | 15 | 20 | - | 1.0 |

For the economic parameters in cost evaluation, hot and cold utility cost are 115.2 \$/kW.yr and 1.3 \$/kW.yr, respectively. Annualization factor is 0.2 which corresponds to 10 years of project life time and 15% prevailing rate of interest. The exchanger minimum approach temperature (EMAT) is 5°C. The capital cost of heat exchanger is calculated using Eq. 4.31.

$$\text{Heat exchanger cost} = C_f + C_A(\text{Area})^B \quad (4.31)$$

Where C_f is fixed cost of heat exchanger = 8333.3 \$/exchanger and C_A is area cost = 641.7 \$/m^(2B) and B is area exponent = 1.

4.2.3 Results

4.2.3.1 Determining the Best Model for HEN Adaptation

Since there are three modified models can be used to adapt the initial HEN in HEN adaptation step. Firstly, the best model should be investigated. Thus, in HEN synthesis step, one of three periods will be chosen as the controlled variable. The mathematical model was implemented on GAMS 21.4 with DICOPT2x-C (CONOPT3 and CPLEX 9.0) as MINLP solver. The computer platform is Lenovo Y450 with Intel® Core 2 Duo T6400 CPU at 2.0 GHz.

A. Generated Initial HEN

From the case study, the second period (MOR) was designated as a controlled variable to synthesize the initial HEN. Because it represents the average value among every period, it should be suitable to be the controlled data for determining the best model for HEN adaptation step. In Figure 4.2, HEN-2 for MOR was generated by using MINLP single period model.

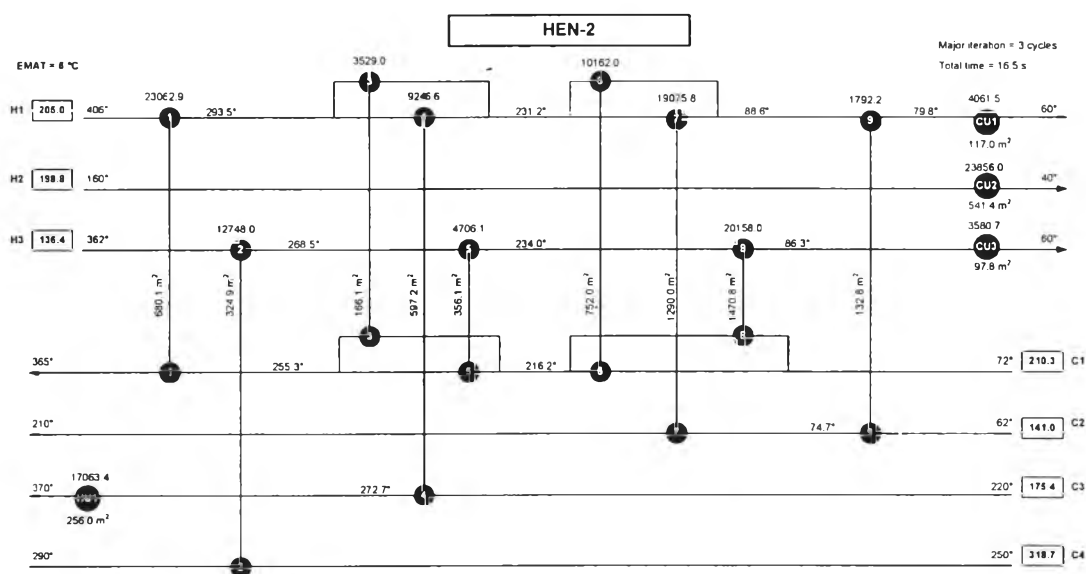


Figure 4.2 Grid diagram of HEN-2.

B. Adapted HENs

Based on initial HEN or HEN-2, it was adapted by entering the some required information of HEN-2 and stream data of period P_1 (SOR) and P_3 (EOR) into the modified models which are model A, B, and C. Some variables such as areas and topology were fixed depending on strategy of each model. Therefore, in this step, there were two more HENs for each modified model (HEN-2-A₁ and HEN-2-A₃ for model A, HEN-2-B₁ and HEN-2-B₃ for model B, HEN-2-C₁ and HEN-2-C₃ for model C). Grid diagrams of adapted HENs are shown in Figure 4.3 to 4.8.

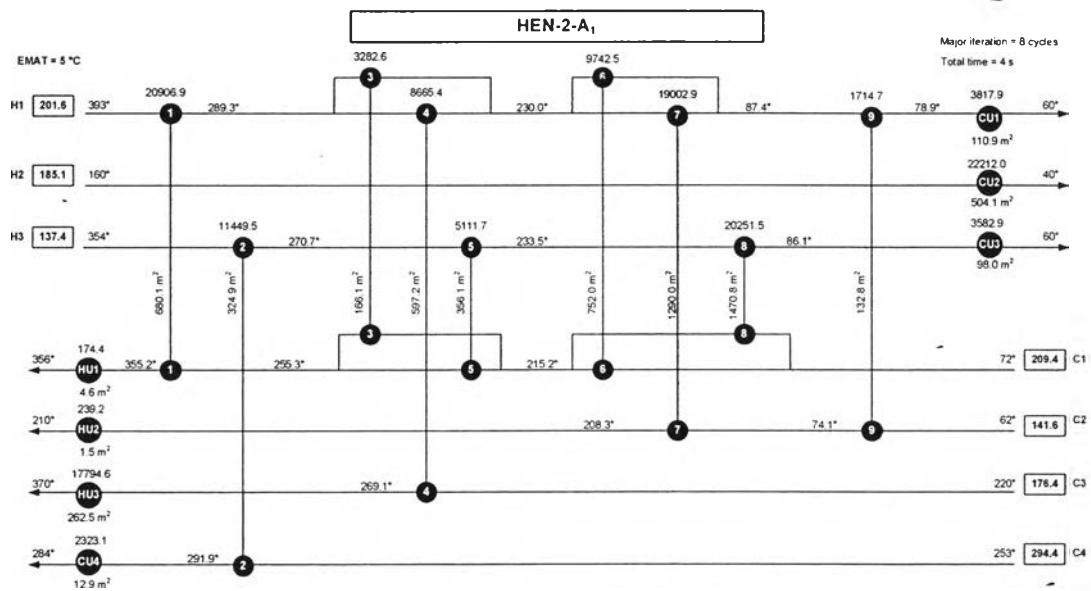


Figure 4.3 Grid diagram of HEN-2-A₁.

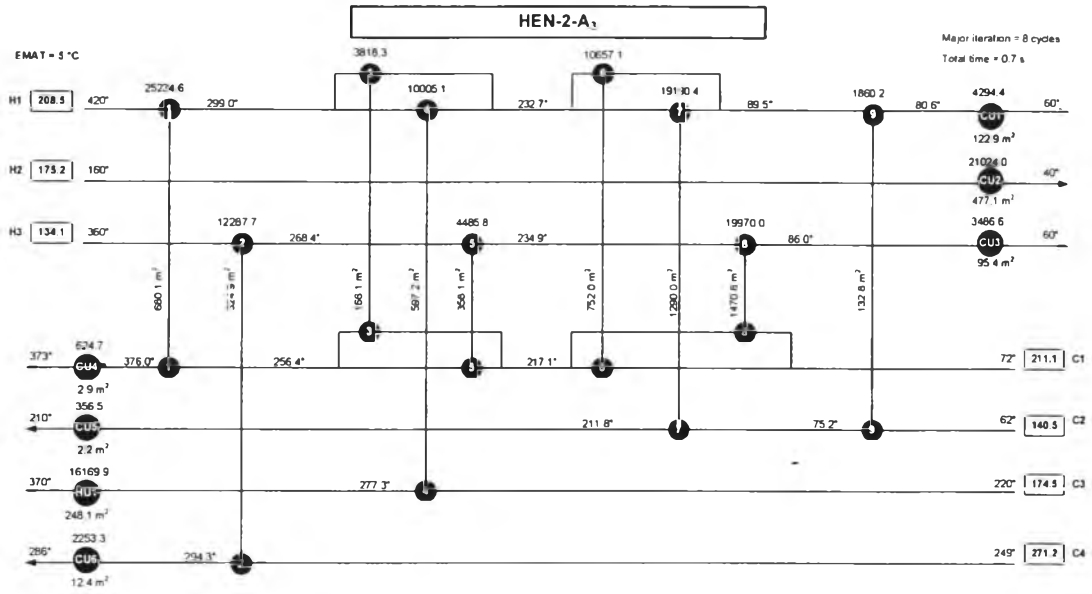


Figure 4.4 Grid diagram of HEN-2-A₃.

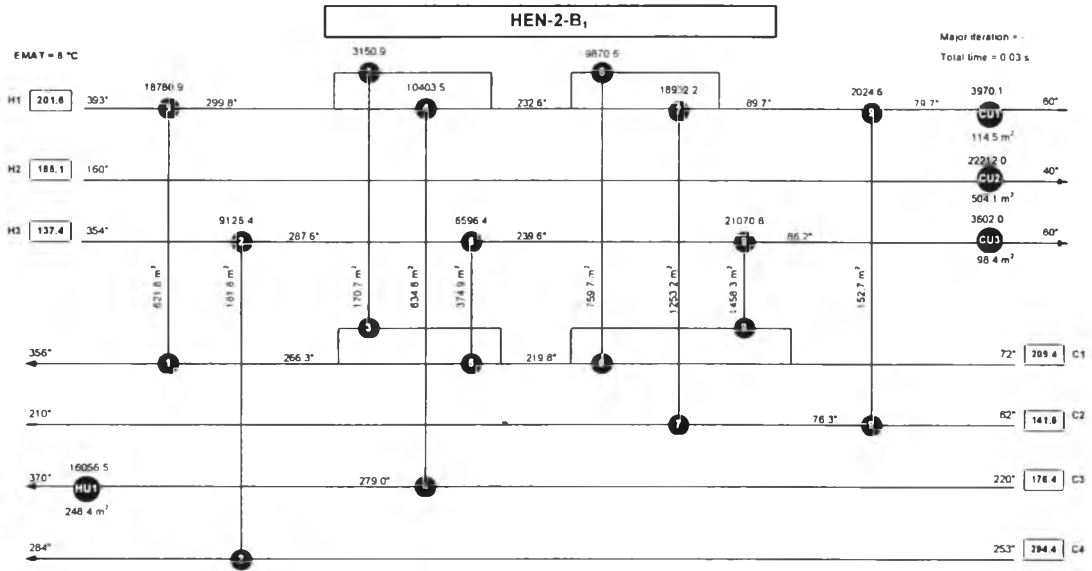


Figure 4.5 Grid diagram of HEN-2-B₁.

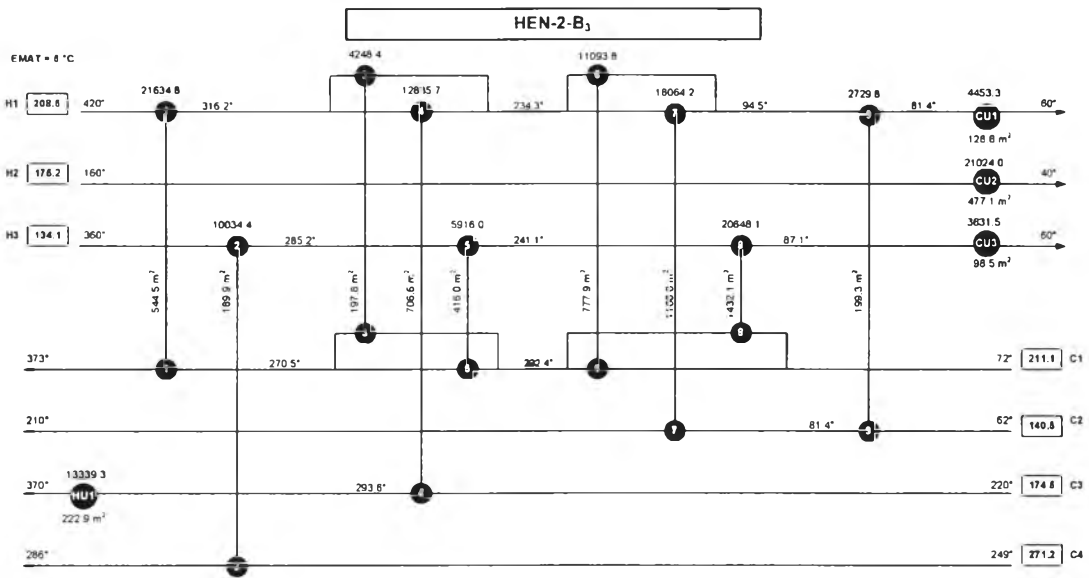


Figure 4.6 Grid diagram of HEN-2-B₃.

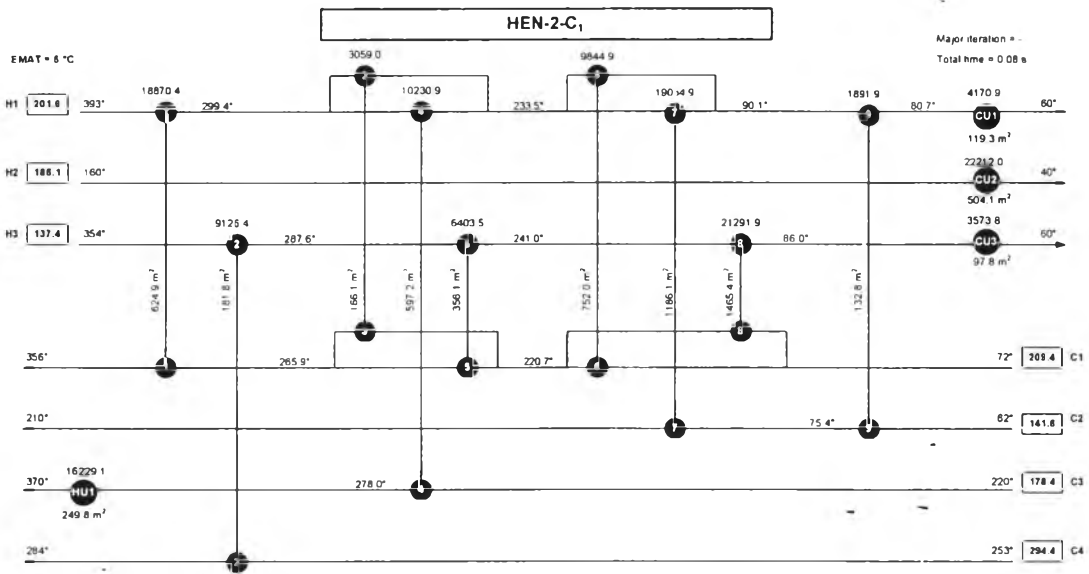


Figure 4.7 Grid diagram of HEN-2-C₁.

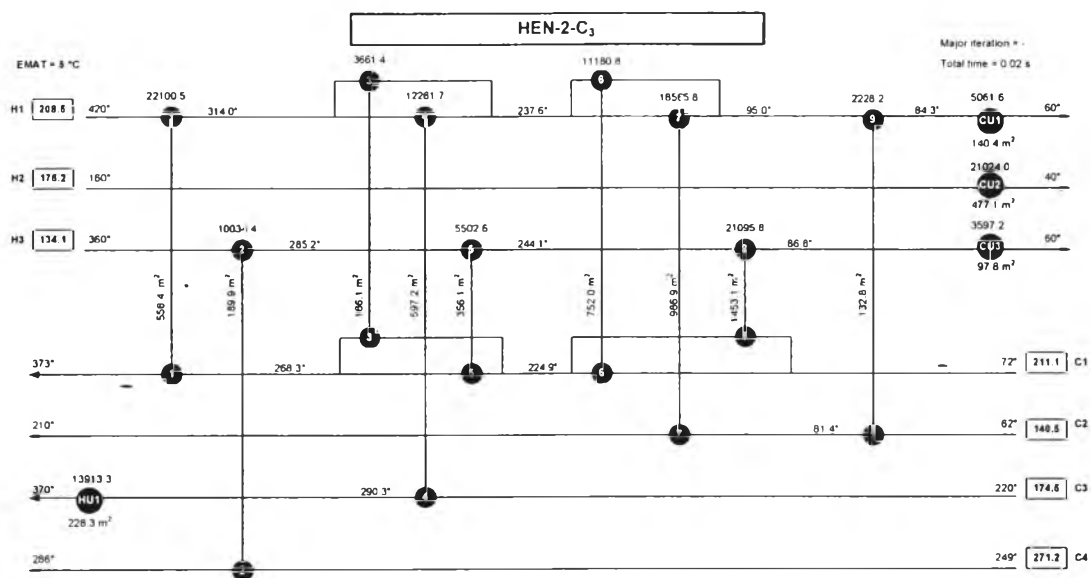


Figure 4.8 Grid diagram of HEN-2-C₃.

C. Integrated HEN

In this step, three HENs for each period of each method will be integrated to get a multiperiod HEN. For example, HEN-2, HEN-2-A₁, and HEN-2-A₃ will be merged by gathering matches that exist in at least one period and maximum area among all periods. The multiperiod HEN-2A, 2B, and 2C are shown in Figure 4.9, 4.10, and 4.11 respectively.

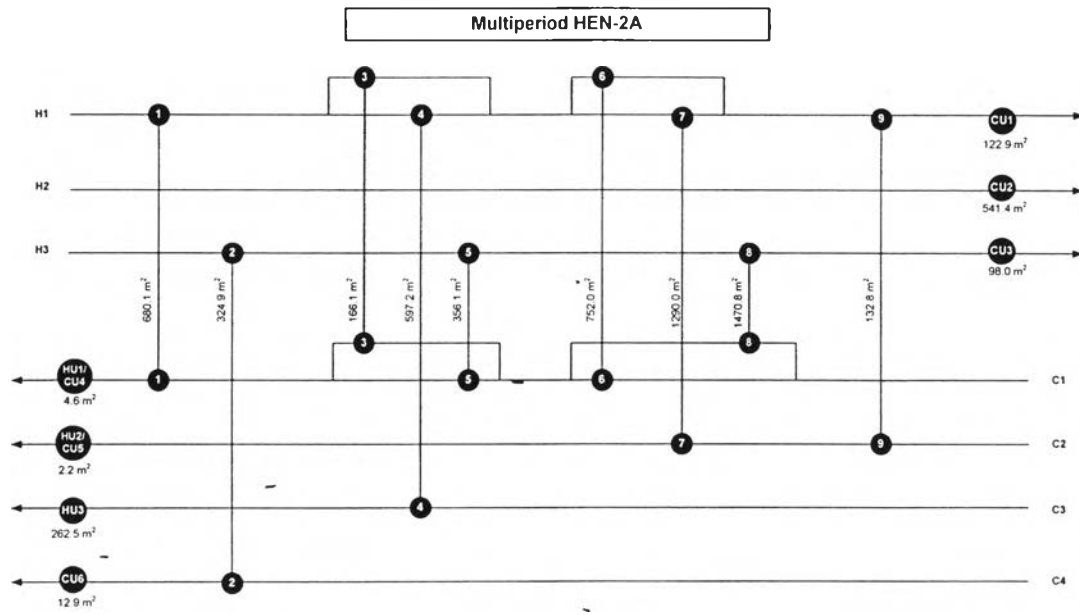


Figure 4.9 Grid diagram of multiperiod HEN-2A.

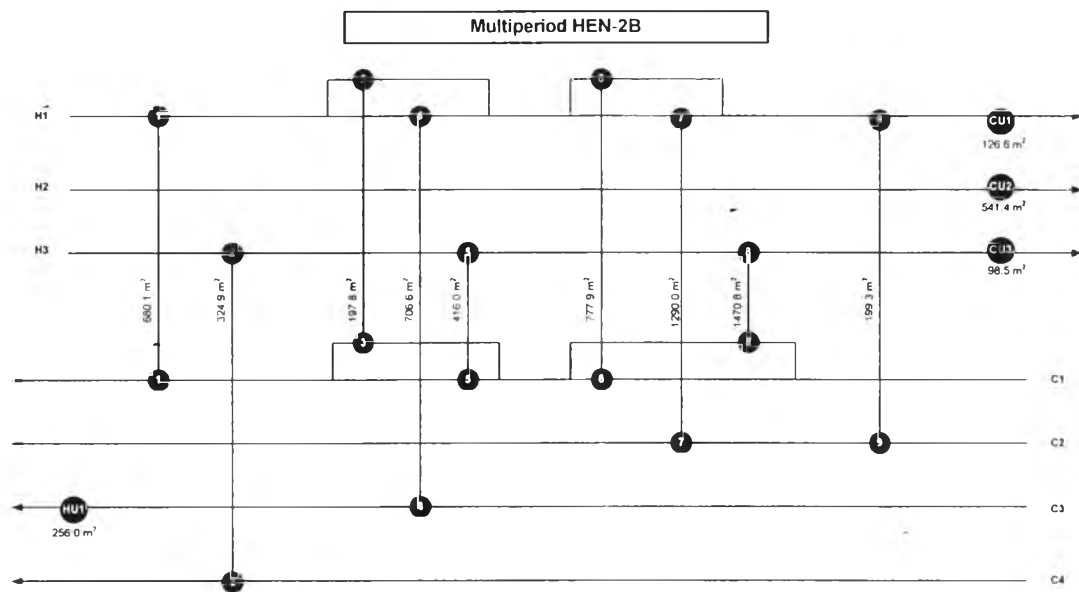


Figure 4.10 Grid diagram of multiperiod HEN-2B.

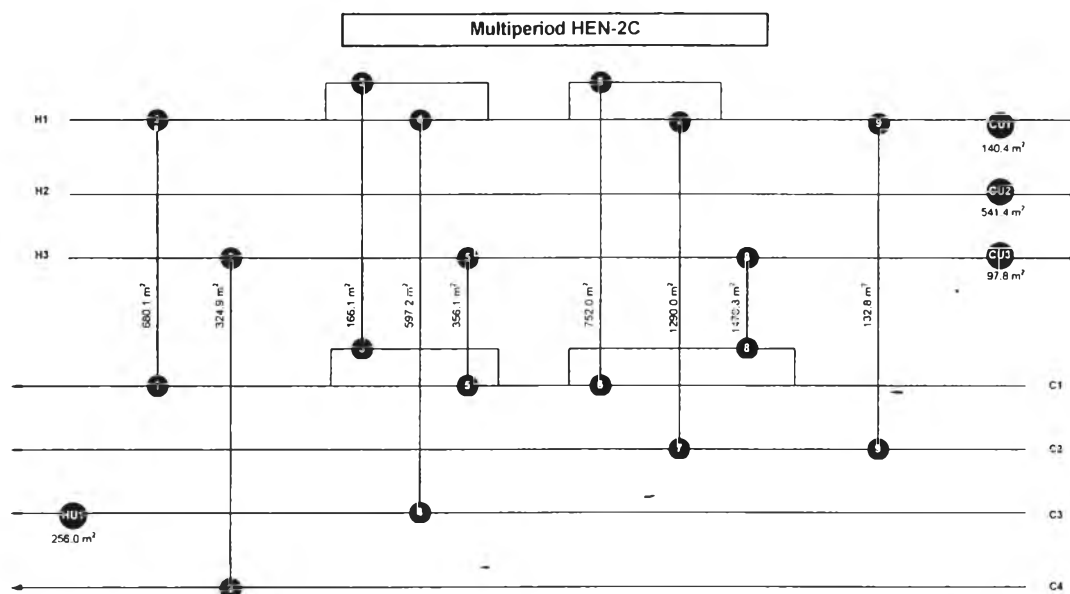


Figure 4.11 Grid diagram of multiperiod HEN-2C.

D. Discussion

Table 4.4 shows the information of multiperiod HEN-2A, 2B, and 2C. It was found that multiperiod HEN-2C, where modified model C was used in HEN adaptation step, gave the lowest TAC at \$2,747,294 per year.

Table 4.4 Results of multiperiod HEN from each method

| | Multiperiod HEN-2A | Multiperiod HEN-2B | Multiperiod HEN-2C |
|------------------------------|-----------------------|-----------------------|-----------------------|
| No. of heat exchangers | 16 | 13 | 13 |
| Total area (m ²) | 6,814.5 | 7,085.8 | 6,805.6 |
| Fixed cost (\$/yr) | 26,666 | 21667 | 21667 |
| Area cost (\$/yr) | 874,573 | 909,397 | 873,432 |
| Utility cost (\$/yr) | 2,011,953 | 1,823,201 | 1,852,195 |
| TAC (\$/yr) | 2,913,193 | 2,754,264 | 2,747,294 |

When using model A for HEN adaptation, it was quite a complex model because of some issues. First, sometimes it might need hot utility in some hot streams and similarly cold utility in some cold streams. This issue should not have occurred because the overall requirement of utility will increase. But this was inevitable because many variables, such as topology and areas of process-process exchangers, were fixed. So the remaining relaxed variables were area and topology of utility exchangers including the types of utility. However, if those nonconventional utility exchangers were not allowed to switch between hot and cold utility, the model would not be able to obtain any feasible solutions. Second, some equations of monotonic temperatures had to be neglected due to the allowance of nonconventional utility exchanger. Moreover, the researcher had to find these nonconventional streams manually because the model cannot find them by itself and it was quite difficult and complicated to identify them.

Model B is more relaxed than model A, hence there is no such nonconventional streams that require the switching of hot and cold utility on the same stream. Since the objective function of model B is least square of area change, the model will try to distribute the change of area to every heat exchanger. Even though the area changes are forced to be as small as possible, the total required area of HEN is more than other models and this causes lowest utility cost. Moreover, it was observed that the areas of heat exchangers are all changed from initial HEN.

Although model C is quite similar to model B, it yielded different solution. It was observed that this objective function would force the model to keep the areas of heat exchangers remain the same value as much as possible. The areas of some heat exchangers would be increased only if it was necessary. So the total area required is lowest, while the utility cost is moderate.

To conclude, model C was the best model for HEN adaptation. Not only because it yielded the lowest TAC when compared to other models, but also there were only some of heat exchangers that needed to be changed while operating. This can be done by bypassing streams when the need of area is lower than the maximum area. And there is also no concern about switching between hot and cold utilities. From these reasons, the sequential approach accompanying model C was the best method to synthesize a robust multiperiod HEN.

4.2.3.2 *Finding the Best Solution by Applying Sequential Method with the Best Modified Model*

From 4.3.2.1, model C is the most robust modified model for HEN adaptation. In this section, it was applied again, but the chosen period for initial HEN synthesis was varied by every period so that multiperiod HEN-1C, 2C, and 3C were obtained. Finally, one of the multiperiod HENs would be designated as the best multiperiod HEN from sequential approach. The overall procedure is shown in Figure 4.12.

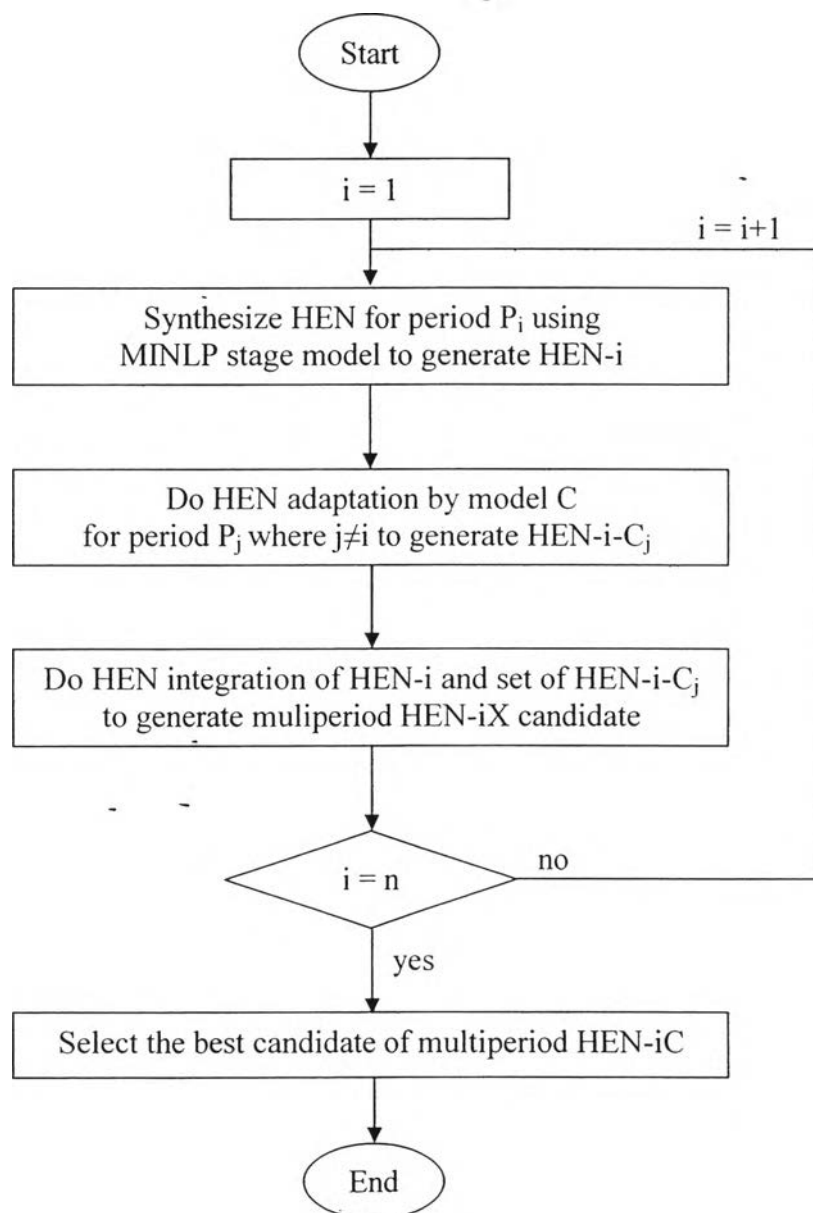


Figure 4.12 Overall procedure of sequential method by using model C.

A. Generated Initial HEN

From case study, all of three periods were separately used as a chosen period for generating initial HEN in the first step. Figure 4.13, 4.14, and 4.15 shows grid diagrams solved by MINLP single period model for period SOR, MOR, and EOR, respectively.

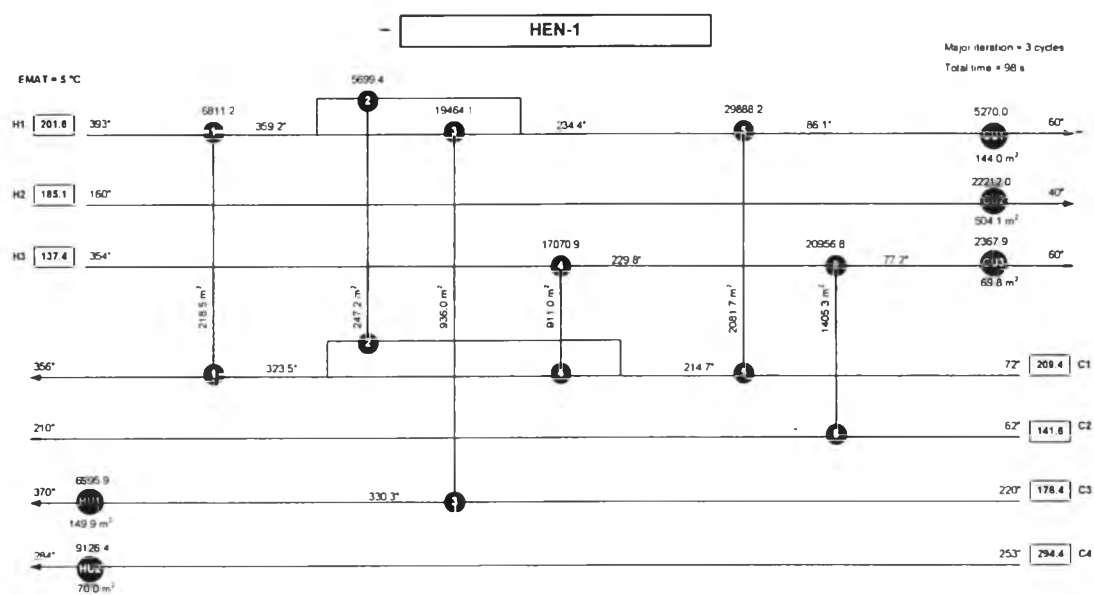


Figure 4.13 Grid diagram of HEN-1.

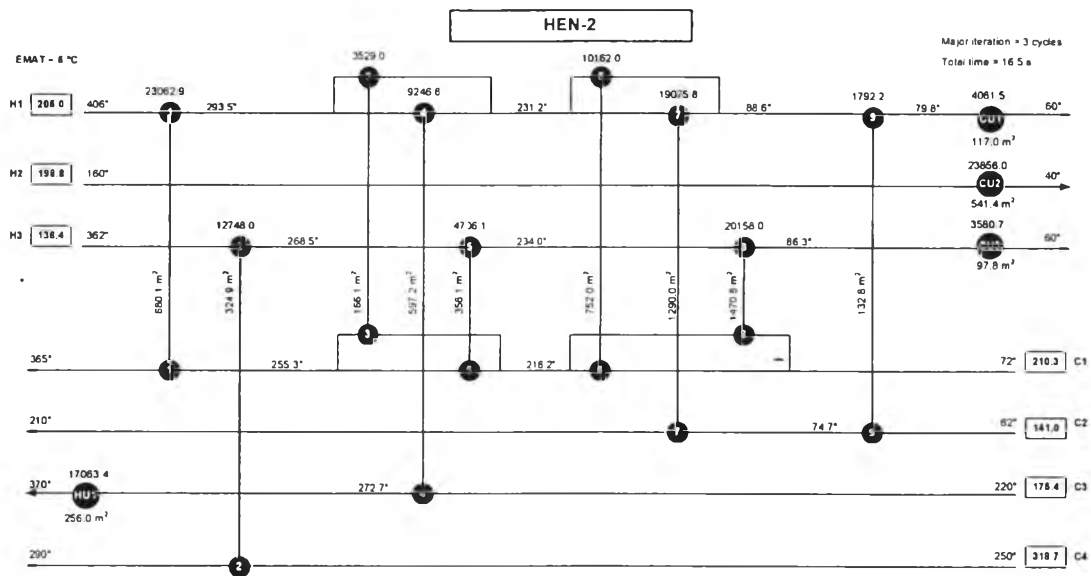


Figure 4.14 Grid diagram of HEN-2.

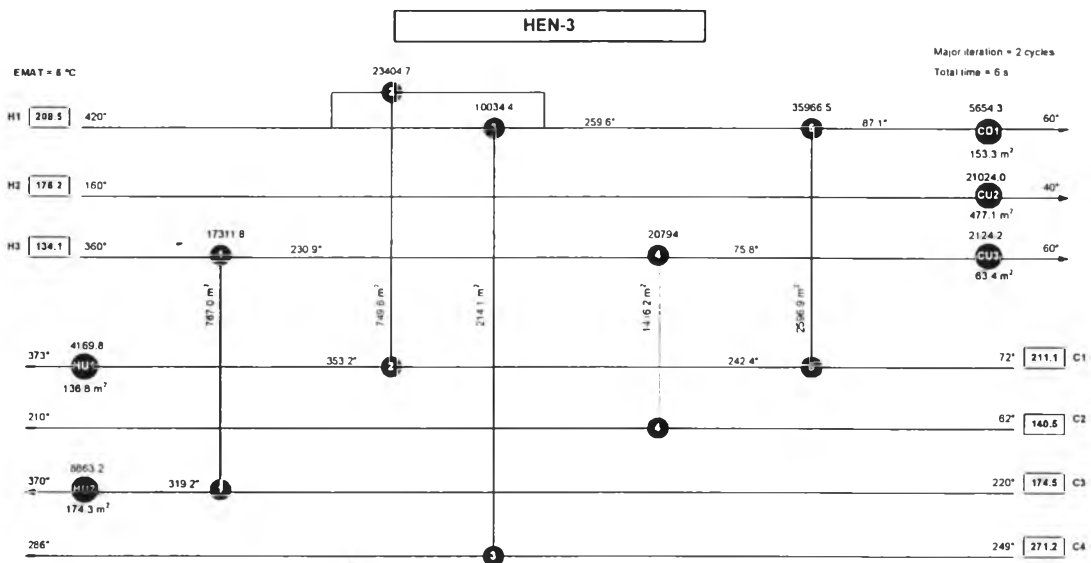


Figure 4.15 Grid diagram of HEN-3.

B. Adapted HENs

From the initial HENs, they were adapted by using modified model C where topology of process exchanger was fixed. The entry of stream properties was from the remaining periods besides the chosen period in HEN synthesis step. For instance, if the chosen period is period 1, the data entry for HEN

adaptation will be period 2 and 3. Therefore, for this case study, there were two more HENs for each chosen period (HEN-1-C₂ and HEN-1-C₃ for period 1, HEN-2-C₁ and HEN-2-C₃ for period 2, HEN-3-C₁ and HEN-3-C₂ for period 3). The grid diagrams of adapted HENs are shown in Figure 4.16 to 4.21.

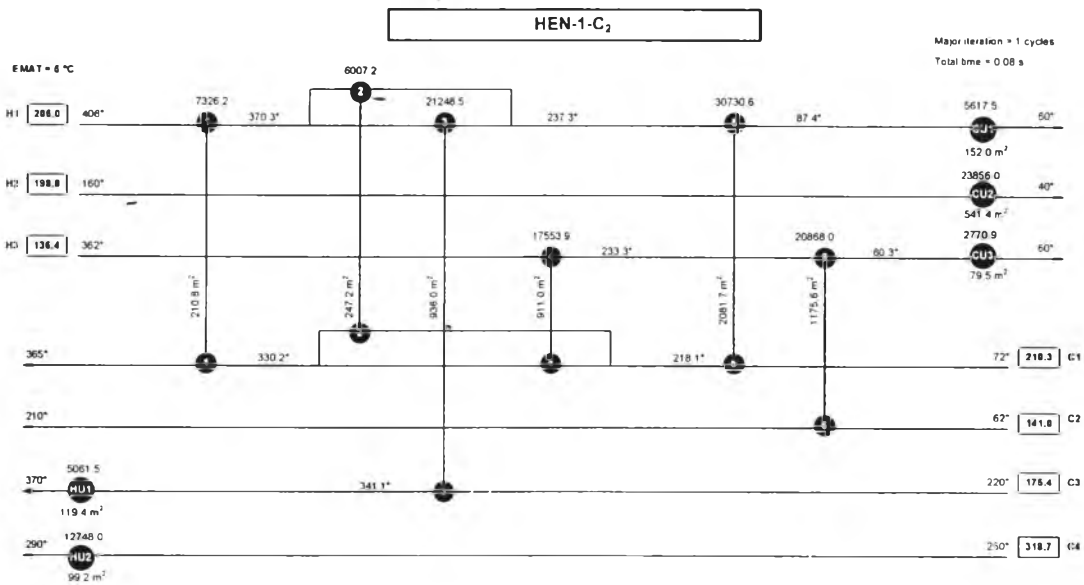


Figure 4.16 Grid diagram of HEN-1-C₂.

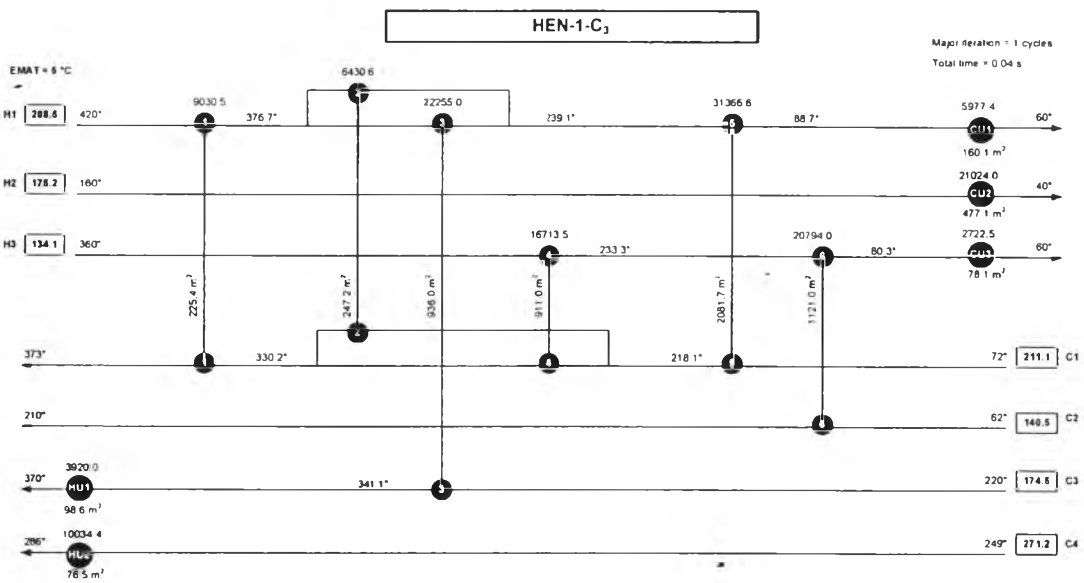


Figure 4.17 Grid diagram of HEN-1-C₃.

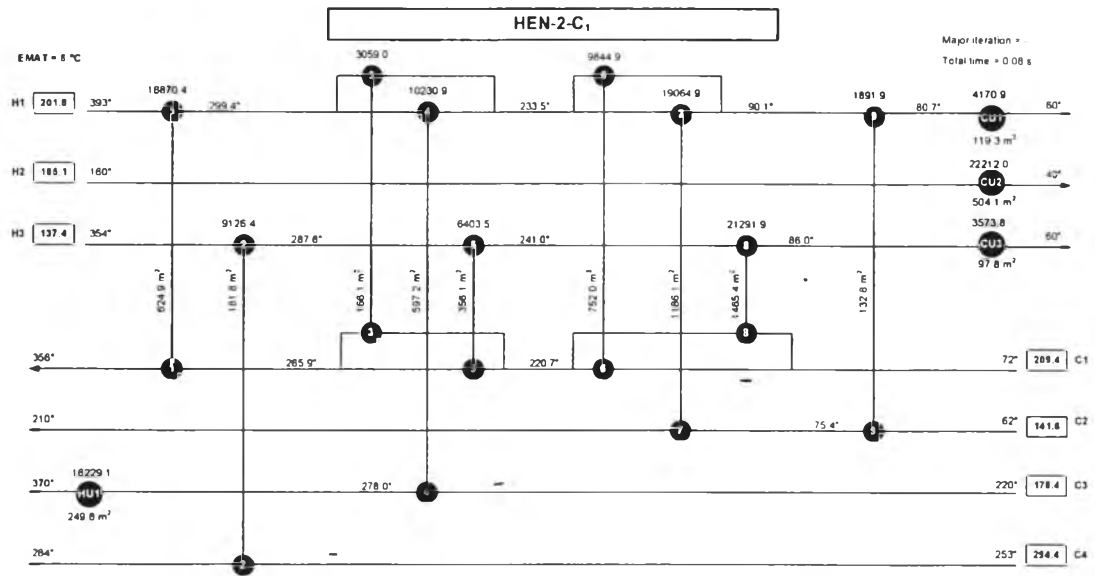


Figure 4.18 Grid diagram of HEN-2-C₁.

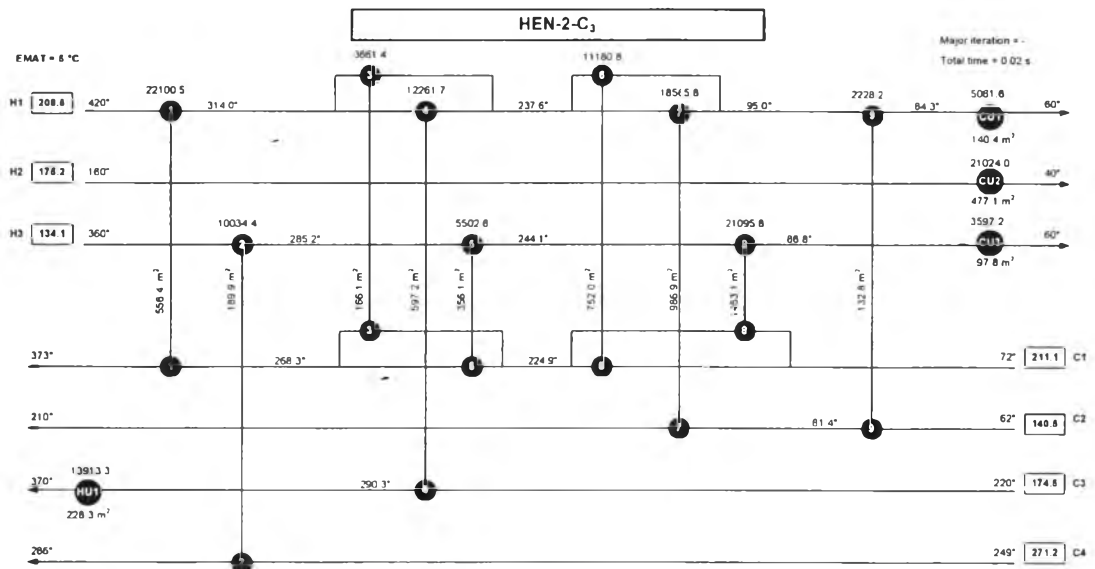


Figure 4.19 Grid diagram of HEN-2-C₃.

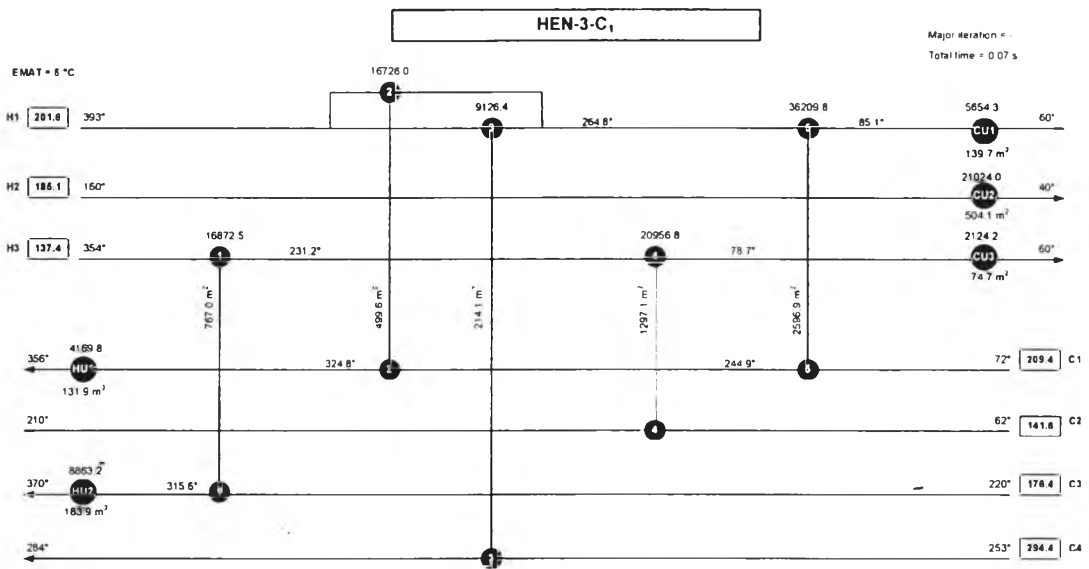


Figure 4.20 Grid diagram of HEN-3-C₁.

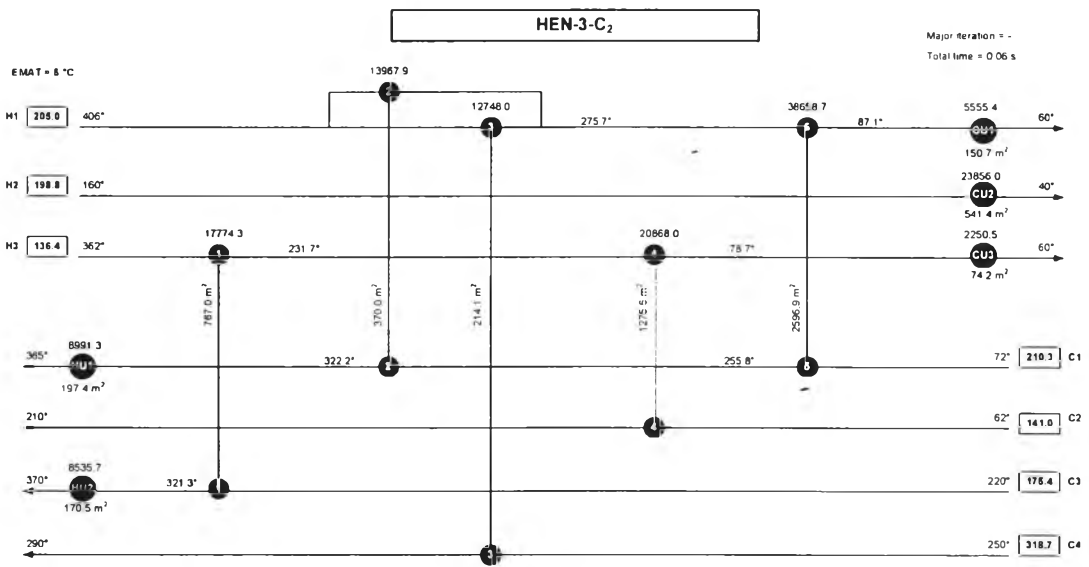


Figure 4.21 Grid diagram of HEN-3-C₂.

C. Integrated HEN

Again, three HENs which based on each chosen period (for instance; HEN-1, HEN-1-C₂, and HEN-1-C₃) were assembled to be multiperiod HEN-iC. The multiperiod HEN-1C, 2C, and 3C are shown in Figure 4.22, 4.23, and 4.24 respectively.

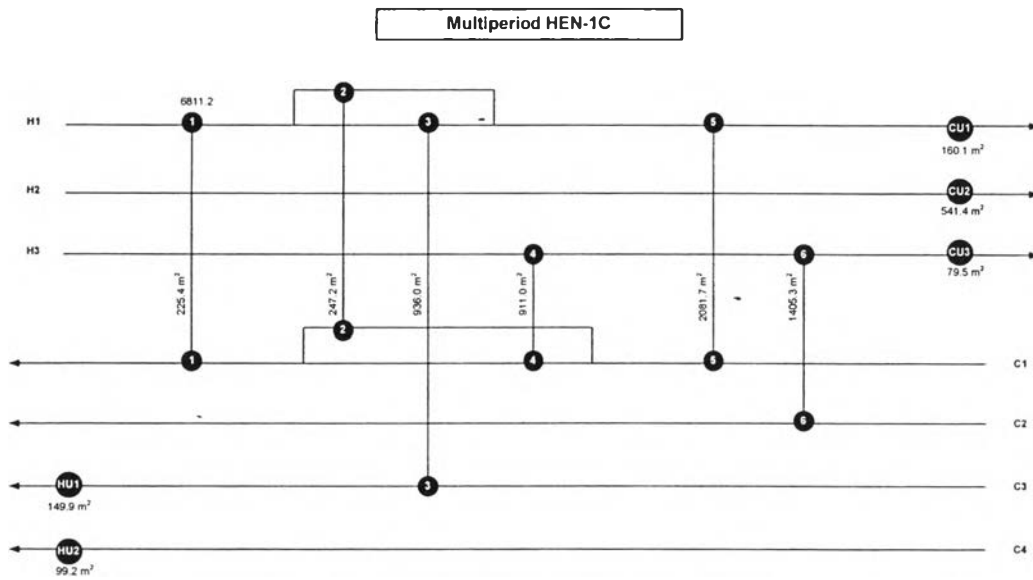


Figure 4.22 Grid diagram of multiperiod HEN-1C.

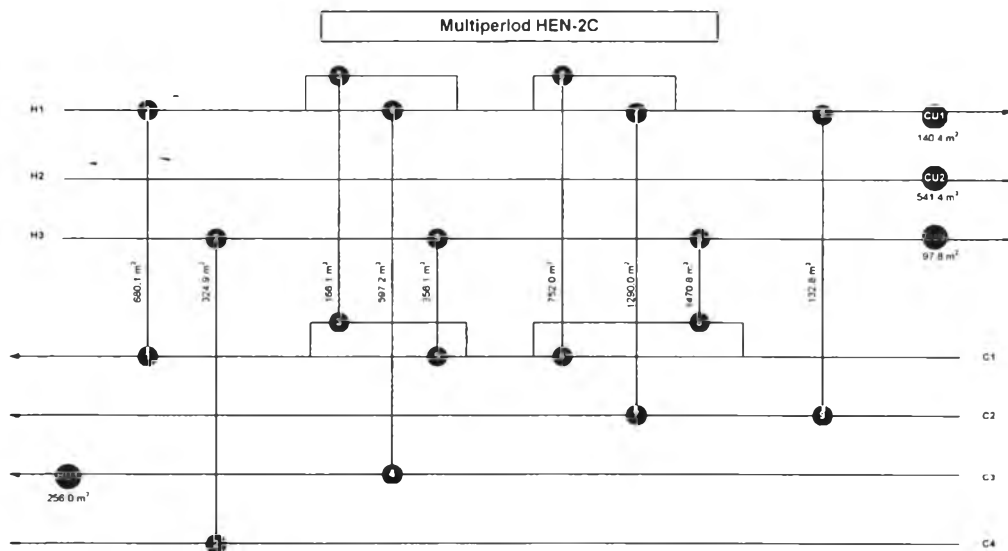


Figure 4.23 Grid diagram of multiperiod HEN-2C.

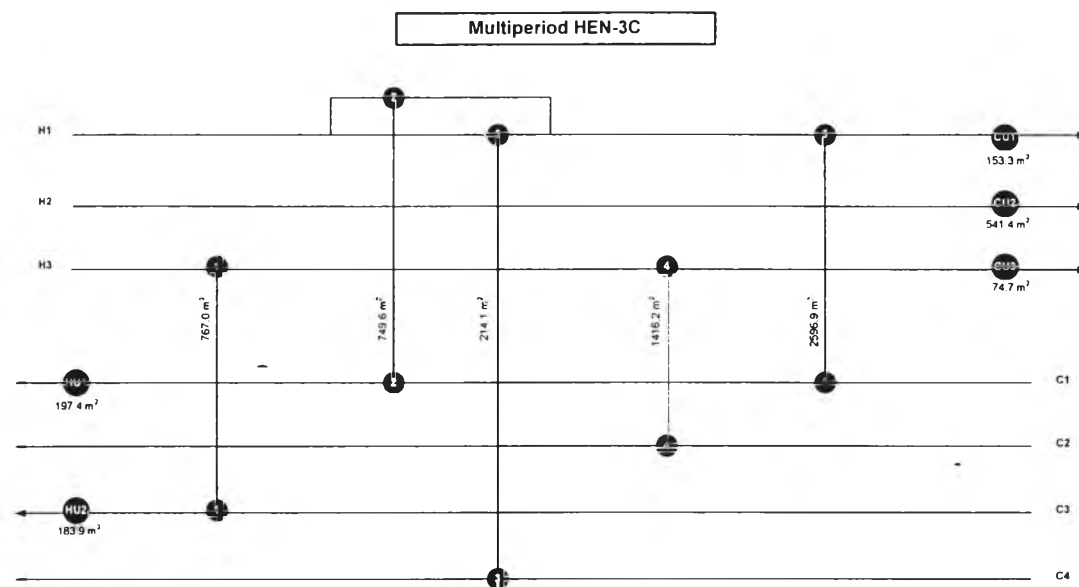


Figure 4.24 Grid diagram of multiperiod HEN-3C.

D. Discussion

Table 4.5 shows the summary information of multiperiod HEN-1C, 2C, and 3C. It was found that multiperiod HEN-3C, where period 3 (EOR) was the chosen period for initial HEN synthesis, yielded the lowest TAC at \$2,733,340 per year.

Table 4.5 Results of multiperiod HEN with different starting period for initial HEN

| | Multiperiod HEN-1C | Multiperiod HEN-2C | Multiperiod HEN-3C |
|------------------------------|-----------------------|-----------------------|-----------------------|
| No. of heat exchangers | 11 | 13 | 10 |
| Total area (m ²) | 6,836.8 | 6,805.6 | 6,894.5 |
| Fixed cost (\$/yr) | 18,333 | 21667 | 16,666 |
| Area cost (\$/yr) | 877,436 | 873,432 | 884,840 |
| Utility cost (\$/yr) | 1,878,620 | 1,852,195 | 1,831,833 |
| TAC (\$/yr) | 2,774,389 | 2,747,294 | 2,733,340 |

It is quite complicated to discuss why using period 3 as the chosen period could give the best solution. There are many relevant factors to be considered.

Firstly, because the utility cost is relatively high when compared to the capital cost; therefore, the network which has lowest utility consumption especially hot utility will tend to have lowest TAC as shown in table 4.5.

Secondly, the efficiency of area usage might have affected the best solution. The efficiency of area usage means how much available area can be used while operating. If the area of heat exchanger from initial HEN design is totally used in other periods, in that case it will have maximum efficiency because there is no need to increase area anymore. In other words, the efficiency means how fit the initial HEN is when it is operated in other periods. However, after calculating the efficiency of area usage, the result is the average efficiency for multiperiod HEN-1C, 2C, and 3C are 96.1%, 94.6%, and 94.3% respectively. Although the efficiency of area usage for multiperiod-3C is lowest, it can still give the best solution. It may be because the effect of utility cost dominates the area cost.

Lastly, the duration of each period should have effect on the best solution. It was anticipated that the period which has longest duration will tend to be more suitable chosen period for generating initial HEN because the network that is based on the longest period will be operate at its maximum efficiency for most of the time. But for this case study, it was assumed that the duration of each period is equal, so it was unable to discuss for this issue.

4.3 Developing a Multiperiod Model for Simultaneous Approach

4.3.1 Formulation of MINLP Multiperiod Model

An MINLP multiperiod model was developed based on stage-wise superstructure model by following the modified model of Verheyen and Zhang (2006) including set of bounding equations. Since the MINLP multiperiod model was developed from MINLP single period model in section 4.1, some modifications were made as follows.

- A. Add set P which is the index for period p.
- B. Input stream properties of every period.
- C. Add P as another dimension for most parameters and variables that depend on period.
- D. Add variables Area_max for representing the maximum area among all periods.
- E. Adjust bounding.
- F. Include equation for determining Area_max.
- G. Change the calculation of utility cost so that it depends on duration of each period.

The MINLP multiperiod model for simultaneous approach consists of a series of equations as shown in Eq. 4.32-4.60.

4.3.1.1 Overall Energy Balance of Each Stream

$$[Th_{in}(i,p) - Th_{out}(i,p)].FCph(i,p) = \sum_{k \in ST} \sum_{j \in CP} q(i,j,k,p) + q_{cu}(i,p)$$

$$i \in HP, p \in PR \quad (4.32)$$

$$[Tc_{in}(j,p) - Tc_{out}(j,p)].FCpc(j,p) = \sum_{k \in ST} \sum_{i \in HP} q(i,j,k,p) + q_{hu}(i,p)$$

$$j \in CP, p \in PR \quad (4.33)$$

4.3.1.2 Energy Balance at Each Stage

$$[th(i,k,p) - th(i,k+1,p)].FCph(i,p) = \sum_{j \in CP} q(i,j,k,p)$$

$$k \in ST, i \in HP, p \in PR \quad (4.34)$$

$$[tc(j,k,p) - tc(j,k+1,p)].FCpc(j,p) = \sum_{i \in HP} q(i,j,k,p)$$

$$k \in ST, j \in CP, p \in PR \quad (4.35)$$

4.3.1.3 Assignment of Inlet Temperatures

$$Th_{in}(i, p) = th(i, 1, p) \quad i \in HP, p \in PR \quad (4.36)$$

$$Tc_{in}(j, p) = tc(i, NOK + 1, p) \quad j \in CP, p \in PR \quad (4.37)$$

4.3.1.4 Monotonic Decrease in Temperatures

$$th(i, k, p) \geq th(i, k + 1, p) \quad k \in ST, i \in HP, p \in PR \quad (4.38)$$

$$tc(j, k, p) \geq tc(i, k + 1, p) \quad k \in ST, j \in CP, p \in PR \quad (4.39)$$

$$th(i, NOK + 1, p) \geq Th_{out}(i, p) \quad i \in HP, p \in PR \quad (4.40)$$

$$TC_{out}(j, p) \geq tc(j, 1, p) \quad j \in CP, p \in PR \quad (4.41)$$

4.3.1.5 Hot and Cold Utility Loads

$$[th(i, NOK + 1, p) - Th_{out}(i, p)]. FCph(i, p) = qcu(i, p) \quad i \in HP, p \in PR \quad (4.42)$$

$$[TC_{out}(j, p) - tc(j, 1, p)]. FCpc(j, p) = qhu(j, p) \quad j \in CP, p \in PR \quad (4.43)$$

4.3.1.6 Logical Constraints

$$q(i, j, k, p) - Q_{up} \cdot z(i, j, k) \leq 0 \quad i \in HP, j \in CP, k \in ST, p \in PR \quad (4.44)$$

$$qcu(i, p) - Q_{up} \cdot zcu(i) \leq 0 \quad i \in HP, p \in PR \quad (4.45)$$

$$qhu(j, p) - Q_{up} \cdot zhu(j) \leq 0 \quad j \in CP, p \in PR \quad (4.46)$$

$$z(i, j, k), zcu(i), zhu(i) \in \{0,1\}$$

4.3.1.7 Minimum Approach Temperature Constraints

$$dt(i, j, k, p) \leq th(i, k, p) - tc(j, k, p) + DT_{up} \cdot (1 - z(i, j, k)) \\ i \in HP, j \in CP, k \in ST, p \in PR \quad (4.47)$$

$$dt(i, j, k + 1, p) \leq th(i, k + 1, p) - tc(j, k + 1, p) + DT_{up} \cdot (1 - z(i, j, k)) \\ i \in HP, j \in CP, k \in ST, p \in PR \quad (4.48)$$

$$dtcu(i, p) \leq th(i, NOK + 1, p) - Tcu_{out} + DT_{up} \cdot (1 - zcu(i)) \\ i \in HP, p \in PR \quad (4.49)$$

$$dthu(j, p) \leq Thu_{out} - tc(j, 1, p) + DT_{up} \cdot (1 - zhu(i)) \\ j \in CP, p \in PR \quad (4.50)$$

4.3.1.8 Log Mean Temperature Difference

$$LMTD(i, j, k, p) = [dt(i, j, k, p) \cdot dt(i, j, k + 1, p) \cdot \frac{dt(i, j, k, p) + dt(i, j, k + 1, p)}{2}]^{1/3}$$

$$i \in HP, j \in CP, k \in ST, p \in PR \quad (4.51)$$

$$LMTDHU(j, p) = \left[dthur(j, p) \cdot dthul(j, p) \cdot \frac{dthur(j, p) + dthul(j, p)}{2} \right]^{1/3}$$

$$j \in CP, p \in PR \quad (4.52)$$

$$LMTDCU(i, p) = \left[dtcur(i, p) \cdot dtcul(i, p) \cdot \frac{dtcur(i, p) + dtcul(i, p)}{2} \right]^{1/3}$$

$$i \in HP, p \in PR \quad (4.53)$$

4.3.1.9 Heat Exchanger Area Calculations

$$Area(i, j, k) = \frac{q(i, j, k, p)}{LMTD(i, j, k, p) \cdot U(i, j)}$$

$$i \in HP, j \in CP, k \in ST \quad (4.54)$$

$$AreaHU(j) = \frac{qhu(j, p)}{LMTDHU(j, p) \cdot UHU(j)}$$

$$j \in CP \quad (4.55)$$

$$AreaCU(i) = \frac{qcu(i, p)}{LMTDCU(i, p) \cdot UCU(i)}$$

$$i \in HP \quad (4.56)$$

4.3.1.10 Determining Maximum Area among all Periods

$$Area_max(i, j, k) \geq Area(i, j, k) \quad i \in HP, j \in CP, k \in ST, p \in PR \quad (4.57)$$

$$AreaHU_max(j) \geq AreaHU(j) \quad j \in CP, p \in PR \quad (4.58)$$

$$AreaCU_max(i) \geq AreaCU(i) \quad i \in HP, p \in PR \quad (4.59)$$

4.3.1.11 Objective Function

$$\begin{aligned} minTAC = AF & \left[\sum_{i \in HP} \sum_{j \in CP} \sum_{k \in ST} C_f \cdot z(i, j, k) + \sum_{i \in HP} \sum_{CU} C_f \cdot zcu(i) \right. \\ & \left. + \sum_{j \in CP} \sum_{HU} C_f \cdot zhu(j) \right] + AF \cdot \sum_{i \in HP} \sum_{j \in CP} \sum_{k \in ST} C \cdot Area_max(i, j, k)^B \\ & + AF \cdot \sum_{j \in CP} C \cdot AreaHU_max(j)^B + AF \cdot \sum_{i \in HP} C \cdot AreaCU_max(i)^B \\ & + \sum_{p \in PR} \frac{DOP(p)}{TOP} \sum_{j \in CP} C_{hu} qhu(j, p) + \sum_{p \in PR} \frac{DOP(p)}{TOP} \sum_{i \in HP} C_{cu} qcu(i, p) \end{aligned} \quad (4.60)$$

4.3.2 Results

The case study is similar to the one that was used in sequential approach. The difference between sequential and simultaneous approaches is that the MINLP multiperiod model of simultaneous method will concurrently solve the problem which has stream properties of all periods. Thus, The HEN adaptation and HEN integration procedures were excluded.

Table 4.6 shows the results of multiperiod HEN synthesized by MINLP multiperiod model and the best HEN from sequential approach in the previous section. And Figure 4.25 shows grid diagram for multiperiod HEN of simultaneous method.

Table 4.6 Comparison of multiperiod HEN from sequential and simultaneous approach

| | Sequential approach (Multiperiod HEN-3C) | Simultaneous approach |
|------------------------------|---|-----------------------|
| No. of heat exchangers | 10 | 10 |
| Total area (m ²) | 6,894.5 | 6,899.7 |
| Fixed cost (\$/yr) | 16,666 | 16,666 |
| Area cost (\$/yr) | 884,840 | 885,515 |
| Utility cost (\$/yr) | 1,831,833 | 1,811,172 |
| TAC (\$/yr) | 2,733,340 | 2,713,354 |

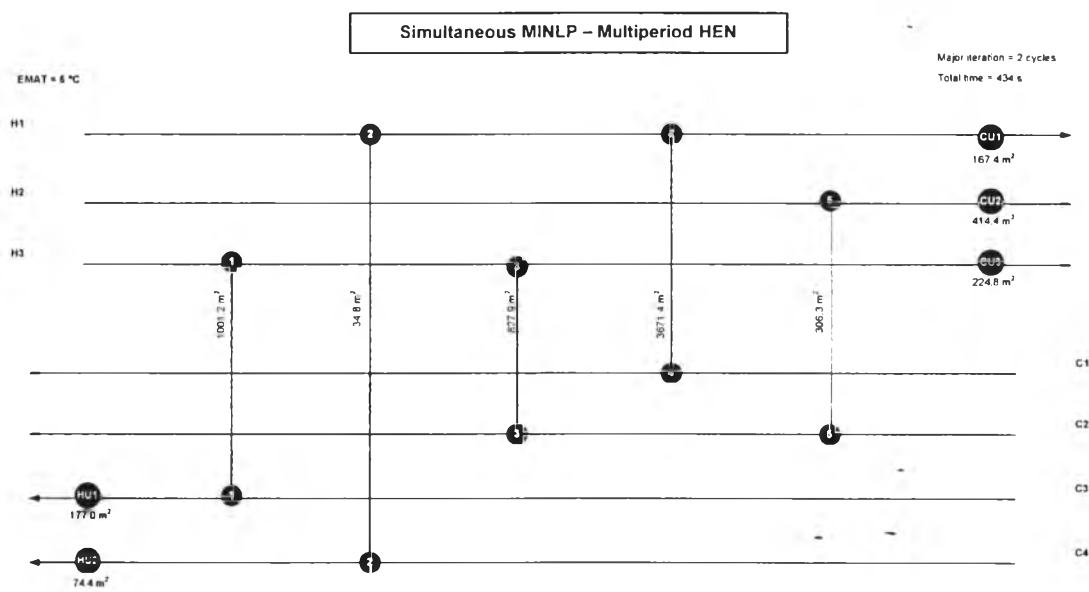


Figure 4.25 Grid diagram of multiperiod HEN synthesized by simultaneous approach.

It was found that the solution from simultaneous approach was better than that of sequential method in term of economy. Because the simultaneous method took into account all of three periods while solving for the optimal multiperiod HEN, thus the obtained network was not trapped in sub-optimal solution

like sequential method. However, this is a small case study, so the objective function of simultaneous approach was improved by just 0.74% when compared to sequential approach. Furthermore, if the structure of HEN in Figure 4.25 was considered, the topology of HEN from simultaneous method was likely to have less complication since there was not any splitted stream in the network, while there was one splitted stream existing in the best HEN from sequential approach.

4.4 Application to Crude Preheat Train in Crude Distillation Unit

Another case study which was carried out to ensure the performance of the proposed method is crude distillation unit in crude oil refinery plant. It is one of the multiperiod problems in chemical processes. Because refinery plants usually purchase various kinds of crude oil from many resources and sometimes blend it together, it will result in different compositions of crude oil. In this study, the simultaneous approach was applied to the case study to synthesize grassroots HEN for crude preheat train. The case study was simulated by using PRO/II with the data taken from Pejpichestakul (2013). After that, the necessary data was collected from the simulation

4.4.1 Case Study Simulation

The simulated case study is crude distillation unit with preflash drum in oil refinery plant. There are total 11 streams comprising of 8 hot streams and 3 cold streams. The CDU operates under three types of service; Troll (light crude), Forozan (medium crude), and Souedie (heavy crude). The crude oil assay data of each crude type is shown in Table 4.7-4.9. The distillation curves or TBP (true boiling point) curves based on the crude assays were plotted as displayed in Figure 4.26.

Table 4.7 True boiling point data of light crude

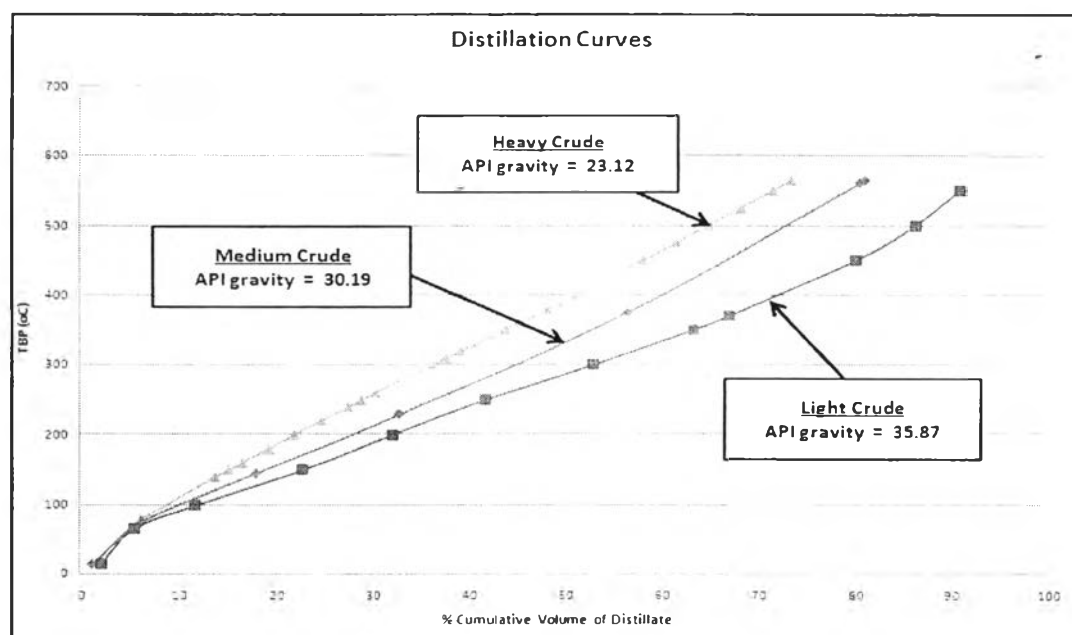
| Percent Distilled | Temperature (°C) |
|-------------------|------------------|
| 2.2 | 15 |
| 5.6 | 65 |
| 11.9 | 100 |
| 22.8 | 150 |
| 32.3 | 200 |
| 41.8 | 250 |
| 53.2 | 300 |
| 63.5 | 350 |
| 67.2 | 370 |
| 80.2 | 450 |
| 86.5 | 500 |
| 91.0 | 550 |

Table 4.8 True boiling point data of medium crude

| Percent Distilled | Temperature (°C) |
|-------------------|------------------|
| 1.3 | 15 |
| 6.3 | 75 |
| 18.0 | 145 |
| 33.0 | 230 |
| 56.8 | 375 |
| 80.6 | 560 |
| 81.2 | 565 |

Table 4.9 True boiling point data of heavy crude

| Percent Distilled | Temperature (°C) | Percent Distilled | Temperature (°C) |
|-------------------|------------------|-------------------|------------------|
| 13.9 | 140 | 43.9 | 350 |
| 15.3 | 150 | 45.4 | 360 |
| 16.7 | 160 | 46.9 | 370 |
| 19.4 | 180 | 48.3 | 380 |
| 22.0 | 200 | 49.8 | 390 |
| 24.7 | 220 | 51.2 | 400 |
| 27.5 | 240 | 58.3 | 450 |
| 29.0 | 250 | 61.7 | 475 |
| 30.4 | 260 | 65.1 | 500 |
| 36.3 | 300 | 68.4 | 525 |
| 37.8 | 310 | 71.7 | 550 |
| 39.4 | 320 | 73.7 | 565 |
| 40.9 | 330 | | |

**Figure 4.26** Distillation curves of each crude oil.

The API gravity data and influent flowrates are shown in Table 4.10. The assay light end composition of each crude oil is shown in Table 4.11.

Table 4.10 Crude used for simulated case study

| Crude | API | Throughput (m ³ /h) |
|--------------|-------|-----------------------------------|
| Light crude | 35.87 | 795 |
| Medium crude | 30.19 | 795 |
| Heavy crude | 23.12 | 795 |

Table 4.11 Light end composition of crude

| Compound | Vol% | | |
|----------|-------------|--------------|-------------|
| | Light crude | Medium crude | Heavy crude |
| Ethane | 0.22 | 0.01 | 0 |
| Propane | 0.58 | 0.28 | 0.07 |
| i-Butane | 0.39 | 0.26 | 0.13 |
| n-Butane | 1.04 | 0.97 | 0.63 |

In the CDU, crude oil is first heated up to 125 °C and then fed to the desalter in order to remove salt in crude oil by dissolving in water. After salt removal, it is heated up again to 170 °C which is the operating temperature of preflash drum. The overhead vapor-phase product from flash drum is fed directly to the distillation column, and the bottom liquid-phase product is further preheated by crude preheat train and furnace to raise the temperature up to 370 °C before entering the fractionation column. Figure 4.27 illustrates the simple flow diagram of CDU with preflash drum.

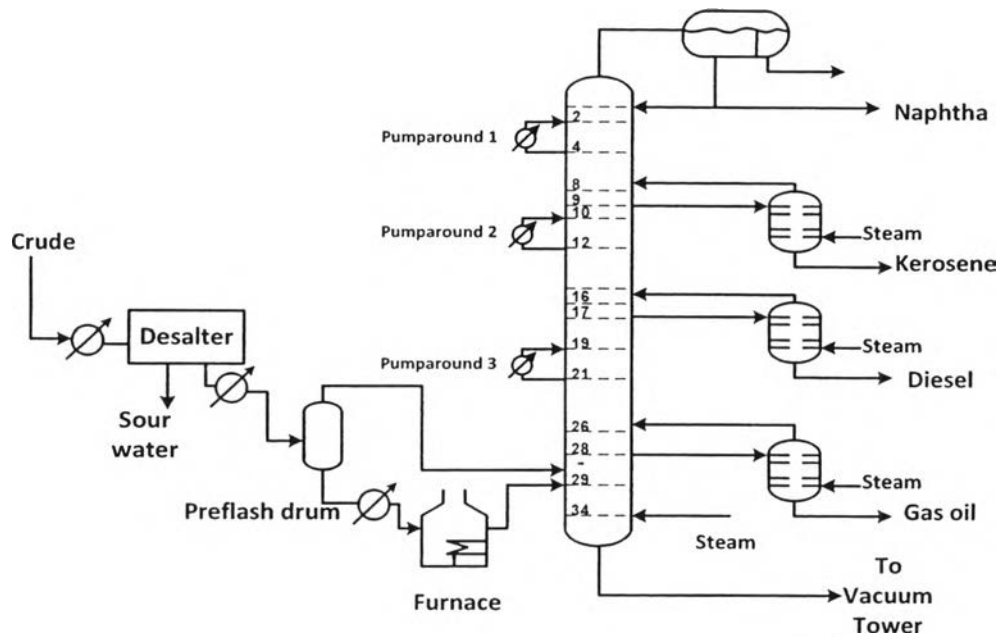


Figure 4.27 The crude distillation unit with preflash drum.

For the column specification, products are specified by using ASTM D86 (5-95 gap and 95% point). The product specification data, overflash rate, feed tray, and withdrawal tray are shown in Table 4.12. The locations of draw and return tray for pump-around and side stripper are shown in Table 4.13. The initial value, condenser outlet temperature, heat rate and return temperature of pump-arounds are illustrated in Table 4.14.

Table 4.12 Products specifications

| Product | Specification | Withdrawal tray |
|------------------|-------------------------|-----------------|
| Naphtha | D86 (95%point) = 182 °C | 1 |
| Kerosene | D86 (95%point) = 271 °C | 9 |
| Diesel | D86 (95%point) = 327 °C | 17 |
| AGO | D86 (95%point) = 410 °C | 28 |
| Overflash rate | 0.01 | |
| Kerosene-Naphtha | (5-95) Gap = 17.2 °C | |
| Diesel-Kerosene | (5-95) Gap = 0.6 °C | |
| AGO-Diesel | (5-95) Gap = -3.4 °C | |
| Feed tray | | 29 |
| Total trays | | 34 |

Table 4.13 Column feed and side draw tray information

| | |
|----------------------------------|---------|
| Number of Plates | 34 |
| Number of trays (Side Strippers) | 4 |
| Pump-around 1 (PA1) Draw | Tray 4 |
| Pump-around 1 (PA1) Return | Tray 2 |
| Pump-around 2 (PA2) Draw | Tray 12 |
| Pump-around 2 (PA2) Return | Tray 10 |
| Pump-around 3 (PA3) Draw | Tray 21 |
| Pump-around 3 (PA3) Return | Tray 19 |
| Kerosene Side-Stripper Return | Tray 8 |
| Diesel Side-Stripper Return | Tray 16 |
| AGO Side-Stripper Return | Tray 26 |
| Crude Feed | Tray 29 |

Table 4.14 Column utilities information

| Variable | Value | | |
|--|-------------|--------------|-------------|
| | Light crude | Medium crude | Heavy crude |
| Kerosene Stripper Steam at 260 °C, 4.4 atm (kg/hr) | 522.5 | 832.5 | 818.6 |
| Diesel Stripper Steam at 260 °C, 4.4 atm (kg/hr) | 2616.5 | 2080.6 | 2217.5 |
| AGO Stripper Steam at 260 °C, 4.4 atm (kg/hr) | 2843.0 | 1860.0 | 1696.0 |
| Main Steam at 260 °C, 4.4 atm (kg/hr) | 3493 | | |
| Overflash | 1% | | |
| Condenser Temperature | 32.22 °C | | |
| Pump-around 1 (PA1) Return Temperature | 104.44 °C | | |
| Pump-around 2 (PA2) Return Temperature | 148.89 °C | | |
| Pump-around 3 (PA3) Return Temperature | 232.22 °C | | |
| Pump-around 1 (PA1) Heat Rate | 11.7 MW | | |
| Pump-around 2 (PA2) Heat Rate | 8.8 MW | | |
| Pump-around 3 (PA3) Heat Rate | 8.8 MW | | |

From the simulation, the stream properties were extracted after running completely. Stream properties, which consist of inlet and outlet temperature, heat capacity flowrates, and heat transfer coefficients, are shown in Table 4.15-4.17. The capital cost of heat exchanger is demonstrated in Eq. 4.61.

$$\text{capital cost of heat exchanger (\$)} = 26,460 + 389 * \text{Area}(m^2) \quad (4.61)$$

The process operates 350 working days with the period of 100, 150, and 100 days for light, medium, and heavy crude, respectively. The project life time of 5 years and prevailing rate of interest of 10% were assumed. Hot and cold utility costs are \$134/kW and \$6.7/kW, respectively. The exchanger minimum approach temperature (EMAT) of 5 °C was used.

Table 4.15 Stream properties of light crude (Troll)

| Stream | FC _p (kW/°C) | T _{in} (°C) | T _{out} (°C) | h (kW/m ² .°C) |
|--------|----------------------------|-------------------------|--------------------------|------------------------------|
| H1 | 121.02 | 201.17 | 104.44 | 1.293 |
| H2 | 69.91 | 274.71 | 148.89 | 1.318 |
| H3 | 98.60 | 321.17 | 232.22 | 1.298 |
| H4 | 105.22 | 32.22 | 30.00 | 1.058 |
| H5 | 67.76 | 234.40 | 30.00 | 1.395 |
| H6 | 49.64 | 273.17 | 30.00 | 1.423 |
| H7 | 59.98 | 326.40 | 30.00 | 1.343 |
| H8 | 135.33 | 341.73 | 30.00 | 0.892 |
| C1 | 380.57 | 25.00 | 125.00 | 0.654 |
| C2 | 434.32 | 125.00 | 170.00 | 0.632 |
| C3 | 585.63 | 166.64 | 370.00 | 0.788 |

Table 4.16 Stream properties of medium crude (Forozan)

| Stream | FC _p (kW/°C) | T _{in} (°C) | T _{out} (°C) | h (kW/m ² .°C) |
|--------|----------------------------|-------------------------|--------------------------|------------------------------|
| H1 | 125.28 | 198.28 | 104.44 | 1.092 |
| H2 | 71.80 | 271.63 | 148.89 | 1.235 |
| H3 | 101.36 | 319.12 | 232.22 | 1.270 |
| H4 | 91.92 | 32.22 | 30.00 | 1.253 |
| H5 | 56.28 | 225.57 | 30.00 | 1.394 |
| H6 | 34.77 | 269.78 | 30.00 | 1.431 |
| H7 | 41.91 | 326.26 | 30.00 | 1.413 |
| H8 | 210.12 | 357.39 | 30.00 | 0.888 |
| C1 | 387.57 | 25.00 | 125.00 | 0.652 |
| C2 | 443.70 | 125.00 | 170.00 | 0.630 |
| C3 | 587.80 | 168.84 | 370.00 | 0.782 |

Table 4.17 Stream properties of heavy crude (Souedie)

| Stream | FC _p (kW/°C) | T _{in} (°C) | T _{out} (°C) | h (kW/m ² .°C) |
|--------|----------------------------|-------------------------|--------------------------|------------------------------|
| H1 | 132.07 | 193.31 | 104.44 | 1.075 |
| H2 | 74.03 | 267.77 | 148.89 | 1.221 |
| H3 | 104.43 | 316.69 | 232.22 | 1.270 |
| H4 | 70.57 | 32.22 | 30.00 | 1.309 |
| H5 | 46.81 | 221.36 | 30.00 | 1.393 |
| H6 | 29.33 | 263.57 | 30.00 | 1.438 |
| H7 | 32.46 | 322.00 | 30.00 | 1.419 |
| H8 | 268.65 | 353.52 | 30.00 | 0.826 |
| C1 | 392.24 | 25.00 | 125.00 | 0.651 |
| C2 | 449.76 | 125.00 | 170.00 | 0.630 |
| C3 | 555.77 | 167.81 | 370.00 | 0.780 |

4.4.2 Results

4.4.2.1 HEN Synthesis by Simultaneous MINLP Multiperiod Model

The refinery case study of CDU is relatively larger scale than the adapted case study from Verheyen and Zhang (2006) since it has more process streams and different time in each period. The solution of multiperiod HEN was obtained in 326,667 seconds by using Acer Intel® Core 2 Quad Processor Q6600 (2.4 GHz). The MINLP multiperiod model, which was used to solve this case study, included some additional constraints which are minimum and maximum of both hot and cold utilities required. These equations are quite similar to boundings for total heat load. Thus, they led to the reduction of computational time. The minimum utilities required were obtained by constructing the composite curves of each period by using HRAT (heat recovery approach temperature) equal to 0 °C. For the maximum utilities required were calculated by summing up total enthalpy of hot streams (for cold utility) or cold streams (for hot utility). The composite curves for

each period are shown in Figure 4.28-4.30. The result of multiperiod HEN for crude preheat train was demonstrated by grid diagram as illustrates in Figure 4.31.

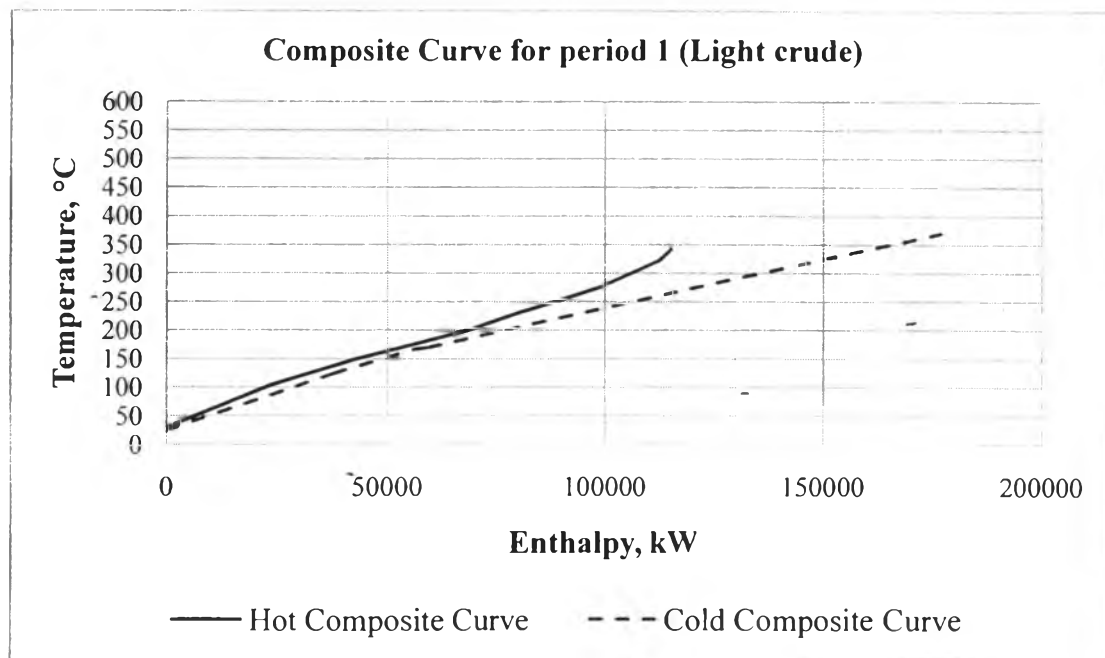


Figure 4.28 Composite curves of period 1 (Light crude).

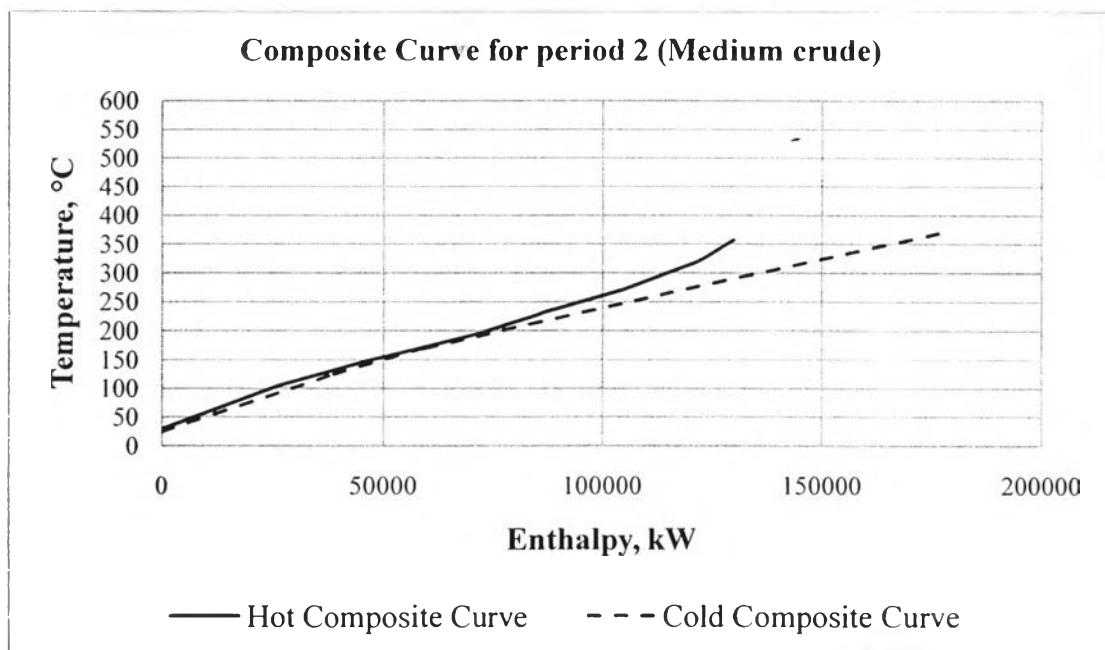


Figure 4.29 Composite curves of period 2 (Medium crude).

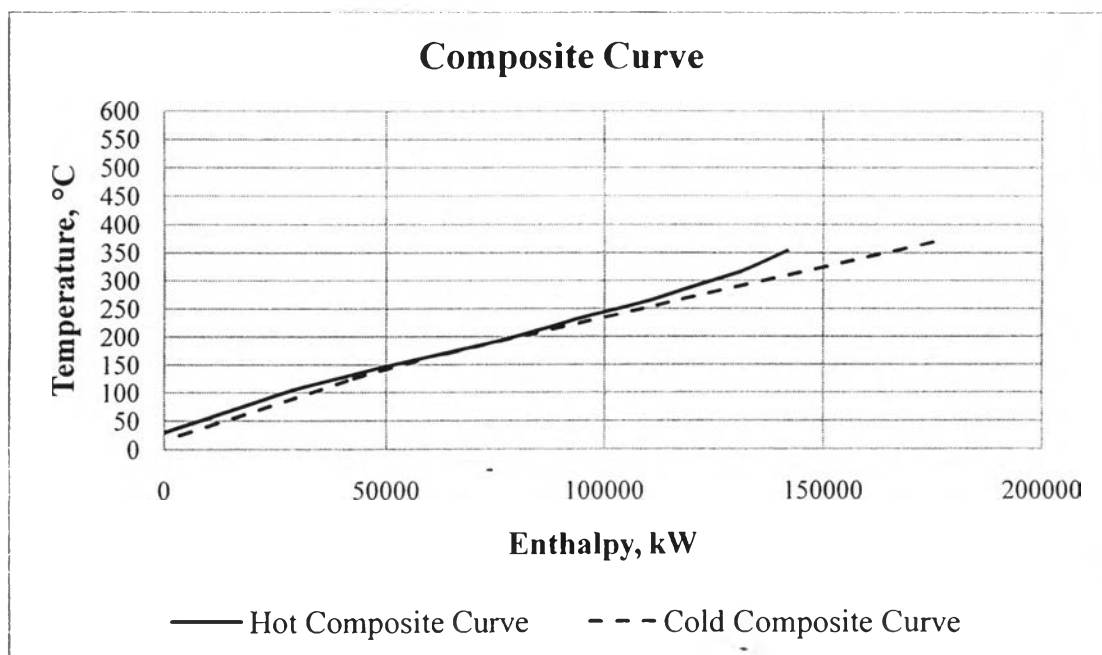


Figure 4.30 Composite curves of period 3 (Heavy crude).

The TAC of multiperiod HEN for the refinery case study was \$9,141,912 per year. There were 21 process exchangers and 8 utility exchangers. The total area of heat exchanger was 15,029 m². It demonstrated that the simultaneous MINLP multiperiod model could perform well and gave a satisfactory solution for large problem. Even though this problem was more complex, it did not require any initial feasible solution before solving. When the computational time was concerned, it spent 644,211 seconds (~ 7.5 days) to solve the problem which has 11 streams. While the small case study of VGO taken from literature with 7 streams spent only 318 seconds to solve. It could be seen that the computational time was considerably sensitive to the number of streams because it caused the number of single equations, single variables, and discrete variables to increase exponentially.

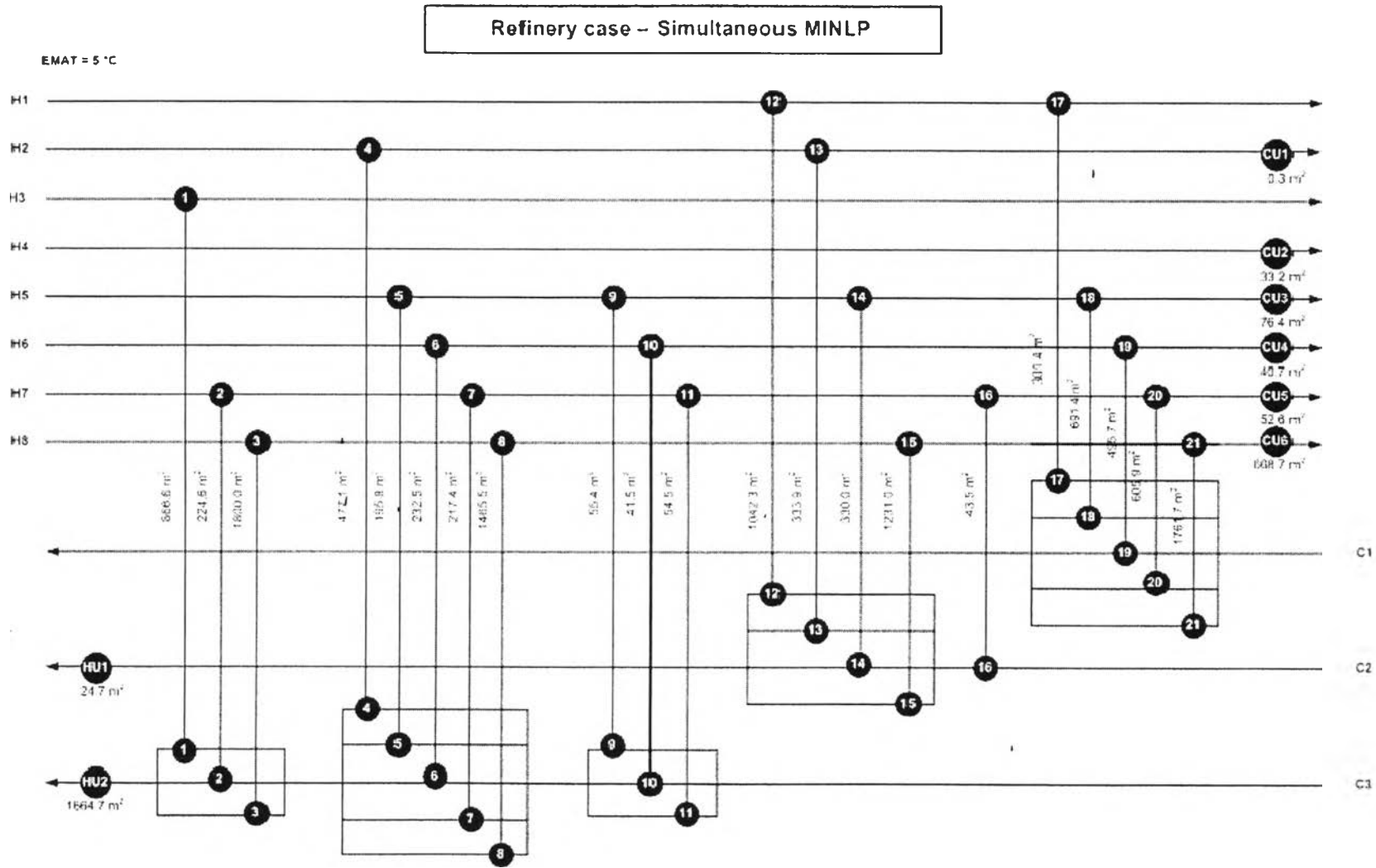


Figure 4.31 Grid diagram of multiperiod HEN for crude preheat train.

4.4.2.2 Model Improvement by Initialization Technique

Due to the overmuch time spent on solving the refinery case study, the initialization technique was adopted. Basically, initialization technique is advantageous to computational time usage and/or solution improvement.

In this study, the principle is to eliminate all nonlinear equations in MINLP multiperiod model so that it becomes an MILP model. Then the MILP model is used to preliminary solve to-obtain rough solution which may close to the optimal solution. This preliminary result from MILP will be use as the initial value for every variable in MINLP multiperiod model. Therefore, the MINLP model will start solving from that initial point instead of beginning with upper and lower bound of each variable.

A. Initialization Strategy

The strategy of initialization technique is to modify all nonlinear equations to linear equations. In the simultaneous MINLP multiperiod model, the area and LMTD (log mean temperature difference) calculation are nonlinear equations. First, in LMTD calculation as illustrated in Eq. 4.62, its nonlinear terms are from the multiplication of temperature differences and the power number of 1/3. These LMTD variables were replaced by constant values which were called average LMTD (ALMTD). Second, for the area calculation as shown in Eq. 4.63, it was considered as nonlinear function because there is a division of variable $q(i,j,k,p)$ by variable $LMTD(i,j,k,p)$. Now that the variables $LMTD(i,j,k,p)$ were replaced by $ALMTD(i,j,p)$; therefore, the area equation would become a linear function.

$$LMTD(i, j, k, p) = [dt(i, j, k, p) \cdot dt(i, j, k + 1, p) \cdot \frac{dt(i, j, k, p) + dt(i, j, k + 1, p)}{2}]^{1/3} \quad (4.62)$$

$$Area(i, j, k) = \frac{q(i, j, k, p)}{LMTD(i, j, k, p) \cdot U(i, j)} \quad (4.63)$$

B. ALMTD calculation Methodology

ALMTD is a constant parameter calculated for each specific match of hot stream i and cold stream j . Firstly, with the assistance of potential program developed by Siemanond and Kosol (2012), optimum HRATs of each period were identified. Secondly, composite curves for each period were plotted with the use of obtained optimum HRAT. Then the composite curves were divided into many temperature intervals (n). In each interval, the LMTD was calculated by using Eq. 4.64 which is real LMTD.

$$LMTD(i, j, k) = \frac{[th(i, k) - tc(j, k)] - [th(i, k + 1) - tc(j, k + 1)]}{\ln \frac{[th(i, k) - tc(j, k)]}{[th(i, k + 1) - tc(j, k + 1)]}} \quad (4.64)$$

For every match of hot stream i and cold stream j , the ALMTDs were obtained by calculating weighted average value of LMTD and heat load (q) in overlapped region as shown in Eq. 4.65.

$$ALMTD(i, j, p) = \frac{\sum_N q(i, j, p, n) \cdot LMTD(p, n)}{\sum_N q(i, j, p, n)} \quad (4.65)$$

C. Results

The ALMTD values of every possible match in each period are shown in Table 4.18 for process-process streams and Table 4.19 for utility-process stream. For the matches which have ALMTD equal to EMAT, it means that those matches have no overlapped zone in the composite curves. However, in real situation, it is impossible for heat to exchange between those matches. Thus, the values of binary variables which indicate the existence for these matches could be preset as 0.

Table 4.18 ALMTD of match between process streams in each period

| Streams | | ALMTD (°C) | | |
|---------|----|---------------------------|----------------------------|---------------------------|
| | | Period 1 (light crude) | Period 2 (medium crude) | Period 3 (heavy crude) |
| H1 | C1 | 22.0 | 23.4 | 27.6 |
| H1 | C2 | 16.8 | 15.7 | 16.3 |
| H1 | C3 | 17.7 | 13.7 | 13.4 |
| H2 | C1 | EMAT | | |
| H2 | C2 | 16.5 | 15.3 | 16.0 |
| H2 | C3 | 28.3 | 22.5 | 18.9 |
| H3 | C1 | EMAT | | |
| H3 | C2 | EMAT | | |
| H3 | C3 | 45.2 | 36.5 | 27.6 |
| H4 | C1 | EMAT | | |
| H4 | C2 | EMAT | | |
| H4 | C3 | EMAT | | |
| H5 | C1 | 19.8 | 23.9 | 30.7 |
| H5 | C2 | 16.8 | 15.7 | 16.3 |
| H5 | C3 | 22.2 | 16.5 | 15.0 |
| H6 | C1 | 19.8 | 23.9 | 30.7 |
| H6 | C2 | 16.8 | 15.7 | 16.3 |
| H6 | C3 | 28.1 | 22.3 | 18.6 |
| H7 | C1 | 19.8 | 23.9 | 30.7 |
| H7 | C2 | 16.8 | 15.7 | 16.3 |
| H7 | C3 | 37.7 | 30.7 | 23.8 |
| H8 | C1 | 19.8 | 23.9 | 30.7 |
| H8 | C2 | 16.8 | 15.7 | 16.4 |
| H8 | C3 | 41.3 | 37.0 | 28.2 |

Table 4.19 ALMTD of match between process stream and utilities in each period

| Stream | Utility | ALMTD (°C) | | |
|--------|---------|---------------------------|----------------------------|---------------------------|
| | | Period 1 (light crude) | Period 2 (medium crude) | Period 3 (heavy crude) |
| H1 | CU | 79.4 | 79.4 | 79.4 |
| H2 | CU | 123.9 | 123.9 | 123.9 |
| H3 | CU | 207.2 | 207.2 | 207.2 |
| H4 | CU | 10.2 | 12.8 | 16.1 |
| H5 | CU | 10.2 | 12.8 | 16.1 |
| H6 | CU | 10.2 | 12.8 | 16.1 |
| H7 | CU | 10.2 | 12.8 | 16.1 |
| H8 | CU | 10.2 | 12.8 | 16.1 |
| HU | C1 | 375.0 | 375.0 | 375.0 |
| HU | C2 | 330.0 | 330.0 | 330.0 |
| HU | C3 | 403.7 | 389.3 | 377.2 |

After executing the modified MILP multiperiod model with these ALMTDs, the solution was taken further to be used as the initial value for MINLP multiperiod model. The grid diagram of generated HEN by MINLP accompanying with initialization is illustrated in Figure 4.32. Its investment cost in TAC was \$9,130,627 per year. There were 21 process exchangers which was equal to the number of process exchanger from HEN without initialization technique. But the number of utility exchanger was only 4 which was less than that from HEN without initialization. The summary results of HEN with and without initialization technique is illustrated in Table 4.20. It demonstrated that the time resource required was decrease substantially by over 70 % when using the initialization strategy. Moreover, it showed that the model with initialization could generate better multiperiod HEN design than that without initialization. The TAC was improved by 0.12 %. It was obviously because the initial value obtained from MILP initialization

model was able to lead the direction of searching algorithm of solver to the better optimal solution due to the use of suitable starting point.

Table 4.20 Summary result of HEN with and without initialization for refinery case study

| Parameter | Without initialization | With initialization |
|------------------------------|------------------------|------------------------|
| No. of heat exchangers | 29 | 25 |
| Total area (m ²) | 15,029 | 16,079 |
| Fixed cost (\$/yr) | 202,578 | 174,636 |
| Area cost (\$/yr) | 1,543,422 | 1,651,209 |
| Utility cost (\$/yr) | 7,395,913 | 7,304,782 |
| TAC (\$/yr) | 9,141,913 | 9,130,627 |
| Time resource (s) | 644,221 (~7.5 days) | 163,433 (~1.9 days) |

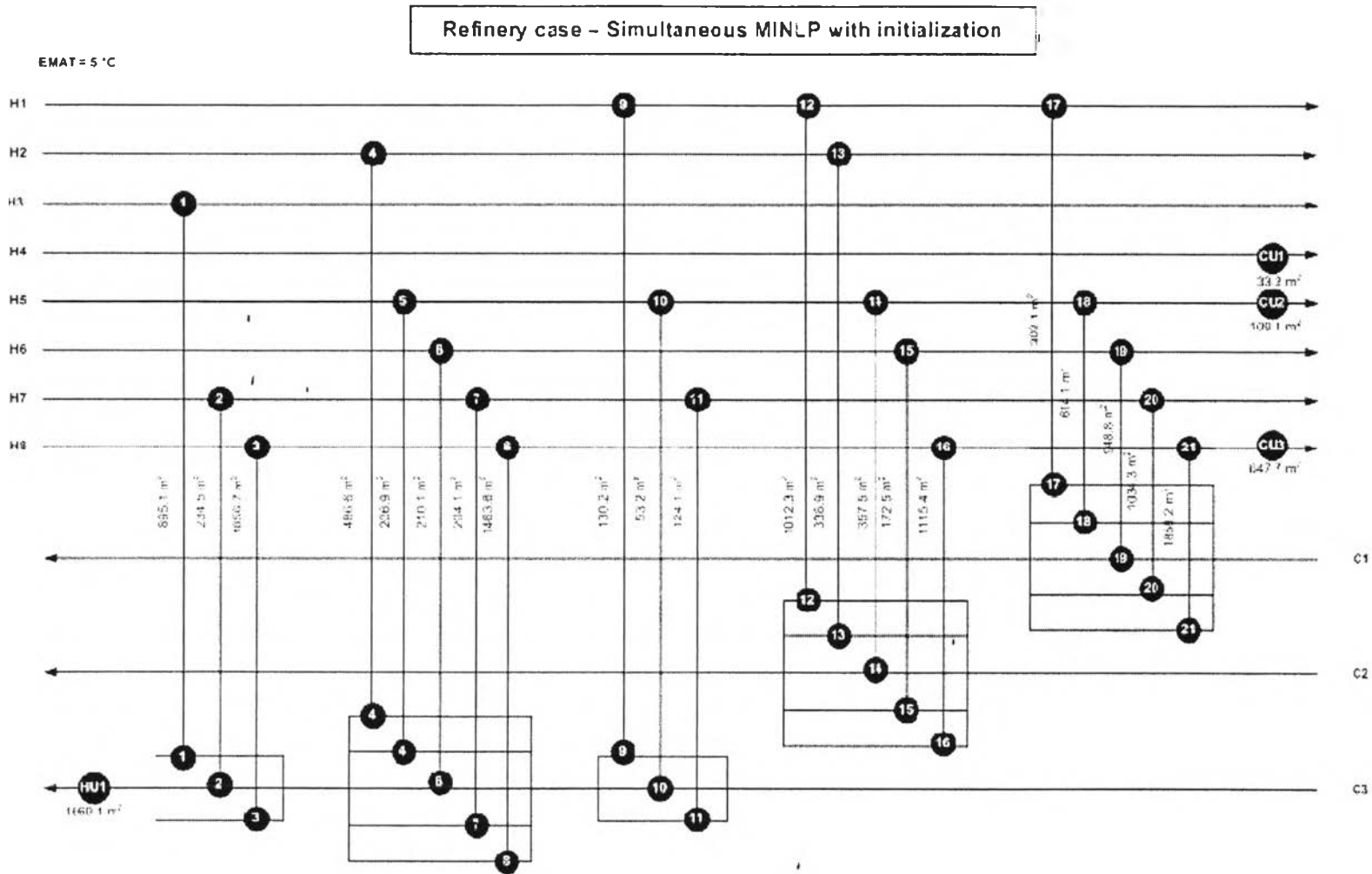


Figure 4.32 Grid diagram of multiperiod HEN for crude preheat train with initialization technique.

In order to confirm the performance of the proposed initialization strategy in term of its benefit to reduce computational time, another implementation of MINLP with initialization technique was carried out. The case study was the same refinery case study except that the time durations for light, medium, and heavy crude were changed to 150, 50, and 150 days, respectively. The summary result is shown in Table 4.21. The time resource required was decreased from 932,021 (without initialization) to 2,337 seconds (with initialization). The reduction of the time resource was even more than the last case study; however, the change of time duration for each period does not relate to the required computational time because it just changes the solution space. From the result, it can be concluded that the proposed initialization strategy could help reduce the computational time considerably with acceptable result of multiperiod HEN. It is possible to obtain better solution by allowing the model with initialization to run for longer time.

Table 4.21 Summary result of HEN with and without initialization for another refinery case study

| Parameter | Without initialization | With initialization |
|------------------------------|------------------------|---------------------|
| No. of heat exchangers | 30 | 22 |
| Total area (m ²) | 15,433 | 15,814 |
| Fixed cost (\$/yr) | 209,563 | 153,680 |
| Area cost (\$/yr) | 1,584,933 | 1,624,078 |
| Utility cost (\$/yr) | 7,396,134 | 7,418,977 |
| TAC (\$/yr) | 9,190,631 | 9,196,735 |
| Time resource (s) | 932,021 | 2,337 |

4.4.2.3 Validation of HEN

The final procedure of HEN synthesis for refinery case study was to validate the best obtained solution and apply back in the process simulation on PRO/II. This step would ensure the feasibility and reliability of the result from the proposed model in the real process. The data of heat exchanger areas and topology were used in the simulation.

Due to the assumption of constant heat capacity flowrates, it was found that some modifications had to be made because the outlet temperature of the process streams, which do not have utility exchangers installed at the end, did not reach the desire temperatures. Hence, some exchanger areas had to be changed by using controller tool in PRO/II to adjust the values of area. Moreover, one utility exchanger was added at the end of stream H3. The final applicable HEN was illustrated in Figure 4.33.

After validation, the TAC was recalculated because the area of some heat exchangers were changed and one more heat exchanger was added into the multiperiod HEN. Table 4.22 shows the new summary result and TAC after validation.

Table 4.22 Summary result of multiperiod HEN after validation

| Parameter | Multiperiod HEN after validation |
|------------------------|-------------------------------------|
| No. of heat exchangers | 26 |
| Fixed cost (\$/yr) | 181,621 |
| Area cost (\$/yr) | 1,498,283 |
| Utility cost (\$/yr) | 729,955 |
| TAC (\$/yr) | 8,979,499 |

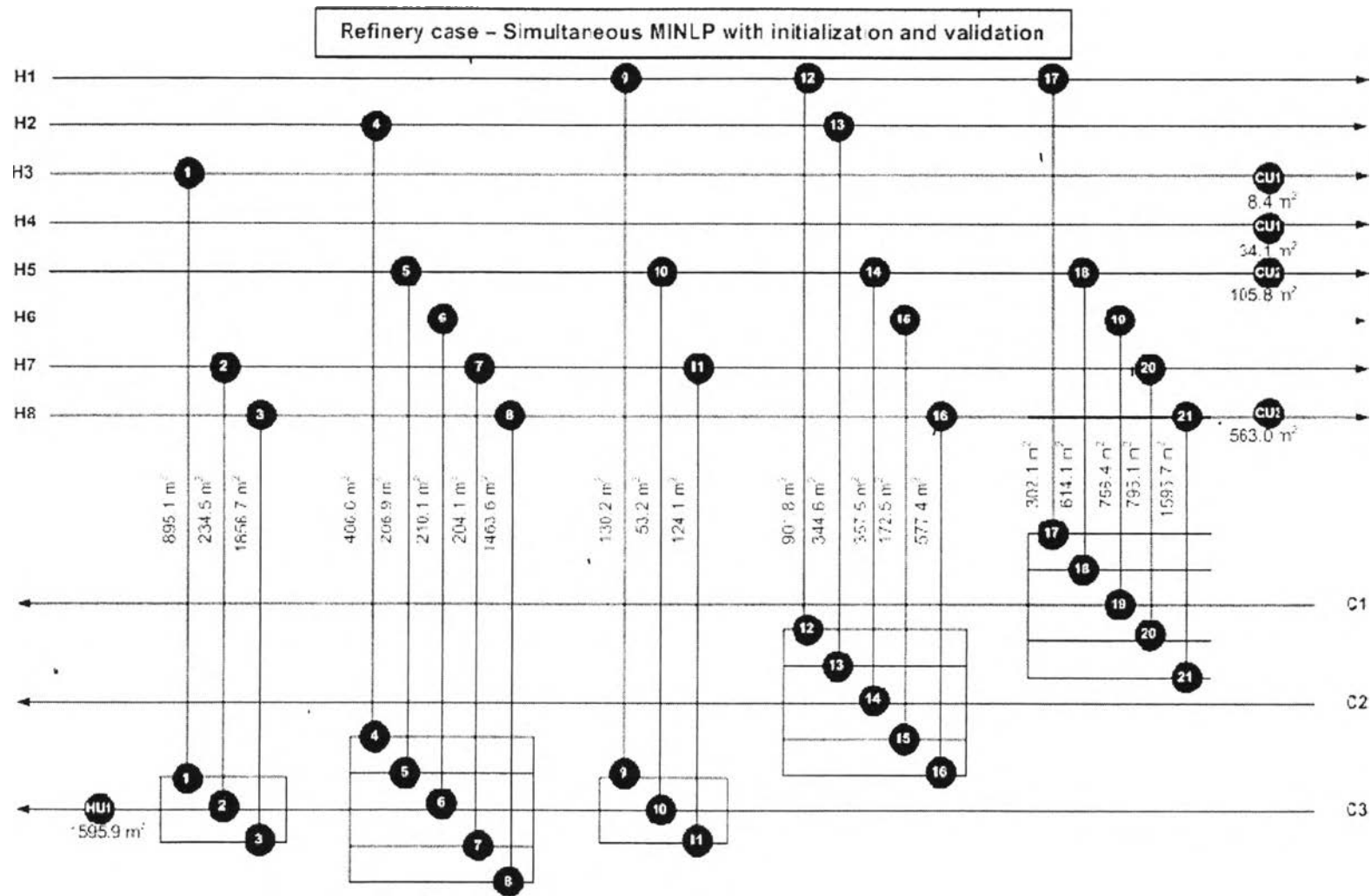


Figure 4.33 Grid diagram of validated HEN for crude preheat train with initialization technique.